

Article

Semi-arid Lakes of Southwestern Siberia as Sentinels of On-Going Climate Change: Hydrochemistry, the Carbon Cycle, and Modern Carbonate Mineral Formation

Andrey Novoselov ¹, Alexandr Konstantinov ², Elizaveta Konstantinova ³, Yulia Simakova ⁴, Artem Lim ², Alina Kurasova ², Sergey Loiko ² and Oleg S. Pokrovsky ^{2,5,*}

¹ Earth Cryosphere Institute, Tyumen Scientific Centre SB RAS, Malygina 86, 625026 Tyumen, Russia; mr.andreygeo@mail.ru

² BIO-GEO-CLIM Laboratory, National Research Tomsk State University, 36 Lenin Ave., 634050 Tomsk, Russia; konstantinov.alexandr72@gmail.com (A.K.); lim_artyom@mail.ru (A.L.); kurasovalina@gmail.com (A.K.); s.loiko@yandex.ru (S.L.)

³ Academy of Biology and Biotechnologies, Southern Federal University, 105/42 Bolshaya Sadovaya Str., 344006 Rostov-on-Don, Russia; konstantliza@gmail.com

⁴ Laboratory of Mineralogy, Institute of Geology of the Komi Science Center of the Ural Branch of the Russian Academy of Sciences, 54 Pervomayskaya Str., 167982 Syktyvkar, Russia; yssimakova@geo.komisc.ru

⁵ Geoscience and Environment Toulouse (GET), UMR 5563 CNRS University of Toulouse, 14 Avenue Edouard Belin, 31400 Toulouse, France

* Correspondence: oleg.pokrovsky@get.omp.eu

Abstract: Towards a better understanding of factors controlling carbon (C) exchange between inland waters and atmosphere, we addressed the inorganic carbon cycle in semi-arid lakes of Central Eurasia, subjected to the strong impact of on-going climate change. As such, we assessed the hydrochemical variability and quantified its control on the formation of authigenic carbonate minerals, occurring within the upper layer of sediments in 43 semi-arid lakes located in the southwest of Western Siberia (Central Eurasia). Based on measurements of pH, total dissolved solids (TDS), cationic and anionic composition, dissolved organic and inorganic C, as well as textural and mineralogical characterization of bottom sediments using X-ray diffraction and scanning electron microscopy, we demonstrate that lake water pH and TDS are primarily controlled by both the lithological and climatic context of the lake watershed. We have not revealed any direct relationships between lake morphology and water chemistry. The most common authigenic carbonates scavenging atmospheric CO₂ in the form of insoluble minerals in lake sediments were calcite, aragonite, Mg-calcite, dolomite and hydromagnesite. The calcite was the most common component, aragonite mainly appears in lakes with sediments enriched in gastropod shells or artemia cysts, while hydromagnesite was most common in lakes with high Mg/Ca molar ratios, as well as at high DIC concentrations. The relationships between mineral formation and water chemistry established in this study can be generalized to a wide suite of arid and semi-arid lakes in order to characterize the current status of the inorganic C cycle and predict its possible modification under on-going climate warming such as a rise water temperature and a change in hydrological connectivity, primary productivity and nutrient regime.

Keywords: lakes; semi-arid region; Western Siberia; inorganic C; CO₂; water chemistry; carbonates



Citation: Novoselov, A.; Konstantinov, A.; Konstantinova, E.; Simakova, Y.; Lim, A.; Kurasova, A.; Loiko, S.; Pokrovsky, O.S. Semi-arid Lakes of Southwestern Siberia as Sentinels of On-Going Climate Change: Hydrochemistry, the Carbon Cycle, and Modern Carbonate Mineral Formation. *Atmosphere* **2023**, *14*, 1624. <https://doi.org/10.3390/atmos14111624>

Academic Editors: Mohamed Hamdi and Kalifa Goïta

Received: 25 September 2023

Revised: 24 October 2023

Accepted: 27 October 2023

Published: 29 October 2023



Copyright: © 2023 by the authors. Licensee MDPI, Basel, Switzerland. This article is an open access article distributed under the terms and conditions of the Creative Commons Attribution (CC BY) license (<https://creativecommons.org/licenses/by/4.0/>).

1. Introduction

The water resources of Central Eurasia, located in the south of Western Siberia and Northern Kazakhstan, within a territory of more than 1,600,000 km² [1], are highly vulnerable in terms of their hydrological regime which is impacted by on-going climate warming. This region is characterized by a specific landscape mosaic, represented by a combination of narrow valleys of large rivers, their tributaries and isolated endorheic (seasonally dried) basins [2]. The hydrological structure of this vast territory, formed by a combination of

geomorphological and climatic factors, predetermined the wide distribution of lakes and ponds—most of them are located within the drainless watersheds [3,4]. The total number of identified lakes (area > 1 km²) in the south of Western Siberia is estimated as more than 20,000. The overall limnicity of the territory ranges between 1 and 10% [5], which is unusually high for the relatively arid region of the world. Small (<1 km²) water bodies are strongly predominant in overall lake number. Most of the small lakes are saline, with overall mineralization higher than 1 g L⁻¹ [6,7]. These lakes are of special interest, because these systems are very sensible to natural and human-induced changes in the climate and transformation of the landscapes. Moreover, saline and hypersaline aquatic environments of drainless basins are potentially important for biodiversity and ecological studies [8]. Further, small water bodies play a disproportionately important role in the terrestrial geochemical cycles of C and related elements [9,10]. A number of recent studies have shown that the role of small lakes and ponds of the arid and semiarid zones in controlling the continental fluxes of elements, notably carbon, is often underestimated [11].

The carbonate system of the lake, including the water column and sediments, is one of the most important factors that predetermines the potential of these water bodies for carbon uptake and storage [12]. The rate of insoluble carbonate mineral formation in lakes is related to a number of parameters including geological and geomorphological context, the hydrochemical composition of waters, hydrological regime, biological activity, as well as the erosional processes within the watersheds [13]. Studies performed for large endorheic lake systems in different arid and semiarid regions of the world have shown that they are characterized by a high degree of intergroup variability in terms of sedimentation processes and authigenic mineral formation [7,14–25]. These studies support the idea that the analyses of the role of endorheic lakes in the formation of regional terrestrial geochemical fluxes primarily requires an understanding of their morphometric diversity taking into account hydrochemical parameters and intensity of C sink in sediments.

The forest-steppe and steppe lakes of Western Siberia are common within a vast territory extending over approximately two thousand kilometers from west to east and are confined to several large geomorphological regions: the Trans-Urals, the Ishim plain, the Barabinsk lowland and the Kulunda plain [7]. The hydrochemical features and sedimentation processes in water bodies of the Trans-Urals and the Ishim plain are much better studied compared to the Barabinsk lowland and the Kulunda plain, though they occupy a significant part of the semiarid part of Western Siberia. Only a few studies were devoted to assessing the composition of waters and bottom sediments of these geomorphological regions with a focus on water bodies, where the formation of authigenic Mg and Mg-Ca carbonates occurs [26–28].

The present study is devoted to assessing the hydrochemical variability of small endorheic water bodies of the Trans-Urals and the Ishim plain geomorphological regions using an example of five groups of lakes, illustrating the gradual physico-geographical transition from Trans-Urals to the inner part of the West Siberian plain. Given that carbon dioxide (CO₂) exchange with the atmosphere and C burial in the form of organic and inorganic carbon are strongly coupled via aquatic photosynthesis, respiration and authigenic carbonate mineral dissolution and precipitation, we focused on assessing the major hydrochemical and mineralogical features of the contrasting and yet representative lakes of the region. Our main objectives were to: (i) evaluate the spatial, morphological and hydrochemical variability of the studied lakes; (ii) analyze the factors affecting the differences in the chemical composition of waters between different groups of lakes; (iii) characterize the typical associations of authigenic carbonates as well as to discuss the possible factors affecting their formation and diversity in sediments. Collectively, these results should enable a better understanding the role of small lakes in the C cycle between the land and the inland water bodies in the context of their strong vulnerability to on-going climate warming in central Eurasia.

2. Materials and Methods

2.1. Geological and Geographical Setting

The studied lakes are located in the forest zone of southwestern Siberia within the territories of the Chelyabinsk, Kurgan and Tyumen regions of Russia (Figure 1). The water bodies are grouped into five key sites that form a transect from the Ural Mountains to the Ishim Plain. In terms of the area of the water surface, 2.3% of the studied lakes are medium water bodies (1–10 km²), 4.6% are small water bodies (0.1–1 km²), and the remaining 93.1% are very small water bodies (<0.1 km²). All studied lakes are rather shallow, with an average depth not exceeding 3 m (Table A1). The duration of the ice cover on studied lakes ranges from 150 to 180 days, depending on the mineralization, size, depth and exact localization within the study territory [26].

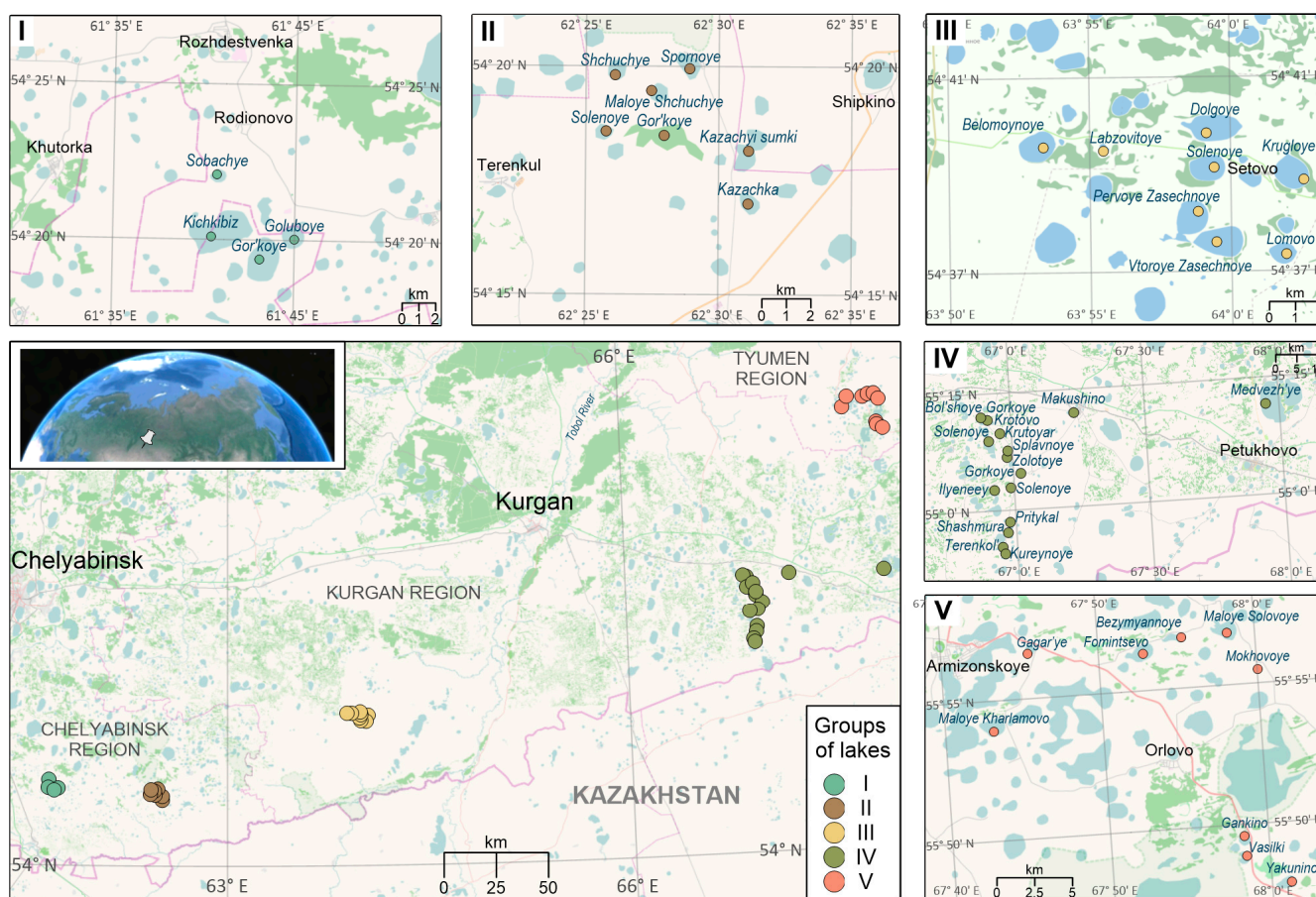


Figure 1. The location of the studied lakes in the southwest of Western Siberia (base maps from www.openstreetmap.org, accessed on 20 August 2023).

The territory belongs to the southwestern edge of the West Siberian Plain, which is a relatively flat area, with <50 m elevation differences and a general slope from south to north and from west to east. The western and the central parts of the territory correspond to the Trans-Ural plain and the eastern to the Ishim plain. The absolute heights decrease from 170–190 m a.s.l. within Chelyabinsk region to 140–150 m within the Kurgan region and 120–130 m within the Tyumen region. The relief of both Transuralian and Ishim plains is weakly dissected, represented by alternating flat watersheds and depressions. The similarity of the geomorphological features of this territory predetermined the wide distribution of drainless basins with lake depression. Suffusion lake depressions are the most common within the discussed area [2].

The river network is poorly developed. Except for the Tobol River valley and its large tributaries, most of the territory belongs to the endorheic basin [2]. The territory under

consideration belongs to the subzone of the forest-steppe. The climate is continental with an annual temperature 2.7–2.9 °C for the Trans-Ural plain and 1.7 °C for the Ishim plain. Annual precipitation varies from 436 mm in the western part of the study area region to 383 mm in the central part and 393 in the eastern [29]. The landscapes of the study territory are significantly transformed by anthropogenic activities, mainly, agriculture. The watersheds are covered with birch groves and plowed fields [30]. The soil cover is represented by Chernozems on the watersheds and Planosols in depressions, which is typical for the West Siberian forest-steppe ecotone [31]. The near-shore zones of saline lakes are often occupied by Solonetz and Solonchak soils [27].

The underlying deposits of the whole studied transect from Trans-Ural plain to Ishim plain are rather similar in terms of genesis and are represented by Quaternary loams of the Uisko-Uboganskaya suite (LIIuu, up to 15 m) and the carbonate loess-like loams of the Ziryansk horizon (LIIIzr). Quaternary deposits are underlain by sandy and loamy strata of the Miocene, Oligocene, and Eocene [32]. The thickness of Quaternary deposits gradually increases with distance from Urals. The aquifers of the study territories are represented by mainly Cretaceous and Eocene-Paleocene marine strata located at a depth of more than 100 m. The underground waters of these horizons are characterized by low mineralization (<1–2 g L⁻¹), chloride-hydrocarbonate composition with a low content of magnesium ions [26].

2.2. Field Work and Sampling

We have sampled 43 water bodies in the Chelyabinsk, Kurgan and Tyumen regions of Russia, representing five groups of lakes that illustrate the gradual transition from the western periphery of the West Siberian plain to its inner part. In total, 43 samples of water and 36 samples of sediments collected during fieldwork periods of 2018–2019 were analyzed in this study (Figure 1, Tables A1 and A2). Sampling field campaigns were mainly conducted in summer and autumn periods corresponding to summer baseflow of the region, which is the main period of authigenic carbonate mineral formation [27,28]. One of the lakes (Zolotoye) was studied in early spring. The two sampled years were within the mean multi-annual air temperature and precipitation. Indeed, mean annual air temperatures of 2018 and 2019 years were 2.1 and 3.3 °C, respectively, while for the historic period of observations the MAAT is 2.9 °C. Mean annual precipitation values of 2018 and 2019 were 343 and 406 mm, respectively, which is comparable with mean mean-multi-annual value of 391 mm. These values have to be considered with caution, given that the study area is rather large and extended; as such, the data obtained at the weather station of the largest regional center (Kurgan) cannot be directly extrapolated to remote parts of the studied territory.

Water samples for chemical analysis were collected from the 40 to 50 cm depth. Temperature (T), pH and total dissolved solids (TDS) were measured in situ using a Multi 3420 portable multiparameter meter (WTW, Xylem Analytics, Germany). The water was filtered on-site through a 0.45 µm membrane filter (MILLEX Syringe Filter unit, Merck, Germany). The first 20–50 mL of filtrate was discarded and the subsequent filtrate was collected into pre-washed 250 mL polypropylene bottles. All the chemical vessels were preliminarily washed and sterilized to prevent contamination. Filtered water samples were taken in two bottles, one was acidified by ultrapure concentrated HNO₃ for the analysis of cations, and the second was not acidified and used for analyses of dissolved organic (DOC) and inorganic (DIC) carbon and anions [33]. Before analyses, filtered samples were stored in a refrigerator at 4–6 °C.

Sediment samples were collected using an Ekman Bottom Sampler. Upper 10 cm of the sediment core were used for laboratory analysis. The sediment samples were air-dried, mixed, ground and passed through a 1 mm sieve for particle size analysis [34].

2.3. Hydrochemical Analysis

Water samples were diluted based on the salinity prior to water chemistry analysis. Concentrations of the major anions (Cl^- and SO_4^{2-}) were analyzed by ion chromatography (Dionex 2000i, Thermo Fisher Scientific, Waltham, MA, USA) with an uncertainty of 2%. The dissolved organic carbon (DOC) and dissolved inorganic carbon (DIC) were determined using a TOC-Vscn analyzer (Shimadzu, Kyoto, Japan) with an uncertainty of 3% and a detection limit of 0.1 mg/L. The samples were diluted by a factor of 3 to 10 prior to analyses. Concentrations of the major cations (Mg^{2+} , Ca^{2+} , Na^+ and K^+) were measured by quadrupole Agilent 7500ce ICP-MS system (Agilent Technologies, Santa Clara, CA, USA) with an uncertainty of $\pm 5\%$. Indium and rhenium were used as internal standards. The international geostandard SLRS-5 (Riverine Water Reference Material for Trace Metals, certified by the National Research Council of Canada) was used to check the validity and reproducibility of each analysis.

2.4. Mineralogical and Textural Analysis

The particle size distribution of sediment samples was analyzed using a laser diffraction analyzer (LS 13 320 Beckman Coulter, Brea, CA, USA), with preliminary sample dispersion in sodium pyrophosphate. Particle size fractions were defined as clay (<0.002 mm), silt (0.002–0.05 mm), and sand (0.05–2.0 mm) according to the USDA particle size classification [35].

The dried samples of sediments were used for mineralogical studies via scanning electron microscopy–energy dispersive spectroscopy (SEM-EDS). The SEM-EDS analysis was performed using a TM3000 scanning electron microscope (Hitachi, Tokyo, Japan) with a Quantax 70 EDS attachment (Bruker, Billerica, MA, USA) at X100–5000 magnification and a JSM-6390LV scanning electron microscope (Jeol, Tokyo, Japan) with an INCA Energy 450 X-Max80 EDS attachment (Oxford Instruments, Abingdon, UK). The SEM observation were made under high vacuum (HV-mode), mainly in the elemental composition mode (BSE, registration of back scattered electrons). While performing the EDS analysis, the voltage was 15 and 20 kV for the first and second devices, respectively.

The semi-quantitative mineralogical composition of the collected sediments was examined by a powder X-ray diffraction (XRD) technique. The analysis was performed with a Shimadzu XRD-6000 diffractometer (Shimadzu, Kyoto, Japan), using $\text{Co-K}\alpha$ -radiation (Ni filter, 30 kV, 20 mA) at a 2θ range from 10° to 60° and a scan speed of 0.03 s^{-1} . Semi-quantitative phase analysis was performed using diffraction patterns of non-oriented samples in the PROFEX program. Corundum standards were always used to constrain the calibration. Analytical uncertainty of the quantification was within 1 wt.%. However, in case of very low content of a given mineral phase in the bulk sample (i.e., 2 to 3%), the uncertainty on its quantification could reach $\pm 100\%$.

2.5. Statistical Treatment and Data Visualization

Calculation of saturation indices of aqueous solution with respect to various carbonate minerals was performed using the Visual MINTEQ ver. 3.1 [36]. The parameters including pH, temperature, and the concentrations of individual ions obtained in situ were used as input parameters.

The software package STATISTICA 12 (StatSoft, Tulsa, OK, USA) was used to analyze data. Basic descriptive statistics included the mean, median, minimum, maximum, standard deviation (SD), and coefficient of variation (CV) for all hydrochemical parameters.

The relationship between the morphometric parameters of the lakes and the hydrochemical properties of the waters was assessed using correlation analysis with the Spearman rank correlation coefficient (significance level $p < 0.05$). The Kruskal–Wallis one-way analysis of variance (ANOVA) by ranks and the median test followed by multiple comparisons of mean ranks for all groups were applied to evaluate differences in hydrochemical properties of the five groups of lakes. Regression analyses were also used to determine the relationship between the main hydrochemical parameters. Data visualization

was performed using Grapher 17 (Golden Software, Golden, CO, USA) and STATISTICA 12 (StatSoft, USA) software.

3. Results

3.1. Water Chemistry

The data on the water chemistry of the studied lakes are listed in Table A2 of the Appendix A. In the summer–autumn season, the water temperature averaged 19.5 °C; the maximum value of 24.9 °C was recorded in September in Lake Solenoye (group III). Water chemistry varied significantly among all studied water bodies (Table 1), which indicates the high degree of heterogeneity, despite of rather similar geological and lithological context. Only in 35% of the studied lakes, the pH values were in the range of 6.5–8.5, which corresponds to a neutral and weakly alkaline reaction. The rest of lakes were characterized by a strongly alkaline solution ($8.9 < \text{pH} < 10.4$). In general, the studied water bodies were characterized by high mineralization; the TDS averaged 26.9 g L⁻¹. Fresh water type (TDS < 1 g L⁻¹) referred to 32.6% of the studied lakes, slightly saline water type accounted for to 4.6% (1–3 g L⁻¹), moderately saline water type amounted to 16.3% (3–10 g L⁻¹), highly saline water type accounted for 16.3% (10–35 g L⁻¹), transitional to brines type constituted 11.6% (35–50 g L⁻¹) and brine type amounted to 18.6% (>50 g L⁻¹). The median concentrations of dissolved major constituents followed the order Na > Mg > K > Ca and Cl > SO₄ > DIC > DOC.

Table 1. Descriptive statistics for main water physicochemical parameters of the semiarid lakes in southwestern Siberia (n = 43).

Parameter	Unit	Mean	Med	Min	Max	SD	CV, %	SE
pH	–	8.7	8.9	6.9	10.4	0.8	8.8	0.1
TDS	g L ⁻¹	26.9	9.8	0.1	160	37.1	138	5.7
Mg ²⁺		1260	233	6	11,200	2260	179	344
Ca ²⁺		103	46.9	7.4	669	147	142	22
Na ⁺		7100	2050	20.1	55,600	11,500	162	1760
K ⁺	mg L ⁻¹	84.9	51	7.5	439	85.9	101	13
Cl ⁻		9510	2270	8.6	83,100	15,800	166	2400
SO ₄ ²⁻		4010	330	0.3	63,900	10,300	258	1600
DOC		80.3	47.1	11.9	1230	182	227	28
DIC		144	101	20	494	116	81	18

The relative ionic composition of water samples representing all studied lakes is plotted on a ternary Piper diagram (Figure 2). According to the ratio of cations, most of the lakes are of the sodium-potassium type. For some water bodies, mainly of group V, the dominant type of cationic composition is not distinguished. According to the anionic composition, most of the lakes of groups I to IV are of the chloride type, while among the lakes of group V, bicarbonate waters predominated. Thus, most of the studied lakes were characterized by sodium chloride waters, some lakes of the V group belonged to the magnesium bicarbonate type.

It should be noted that water chemistry varied widely within the same geographical group, which indicates that the climate and geological context do not have a direct effect for the differentiation of hydrochemical parameters. However, according to the Kruskal Wallis test and the median test, there were significant differences between the mean values of TDS, major ion content, DOC and DIC ($p < 0.005$) in waters belonging to the certain lake group (Table A5). Thus, group III lakes are characterized by maximum median TDS values (42 g L⁻¹), corresponding to increased water salinity, Na⁺ (8900 mg L⁻¹), Cl⁻ (12,000 mg L⁻¹), DOC (91.7 mg L⁻¹), and DIC (309 mg L⁻¹) (Figure 3). In lakes of group I, elevated median values of Mg²⁺ (1400 mg L⁻¹), K⁺ (173 mg L⁻¹), and SO₄²⁻ (3495 mg L⁻¹) are observed. The minimum median values of all studied physicochemical parameters, except for DIC, were characteristic of lakes of the V group.

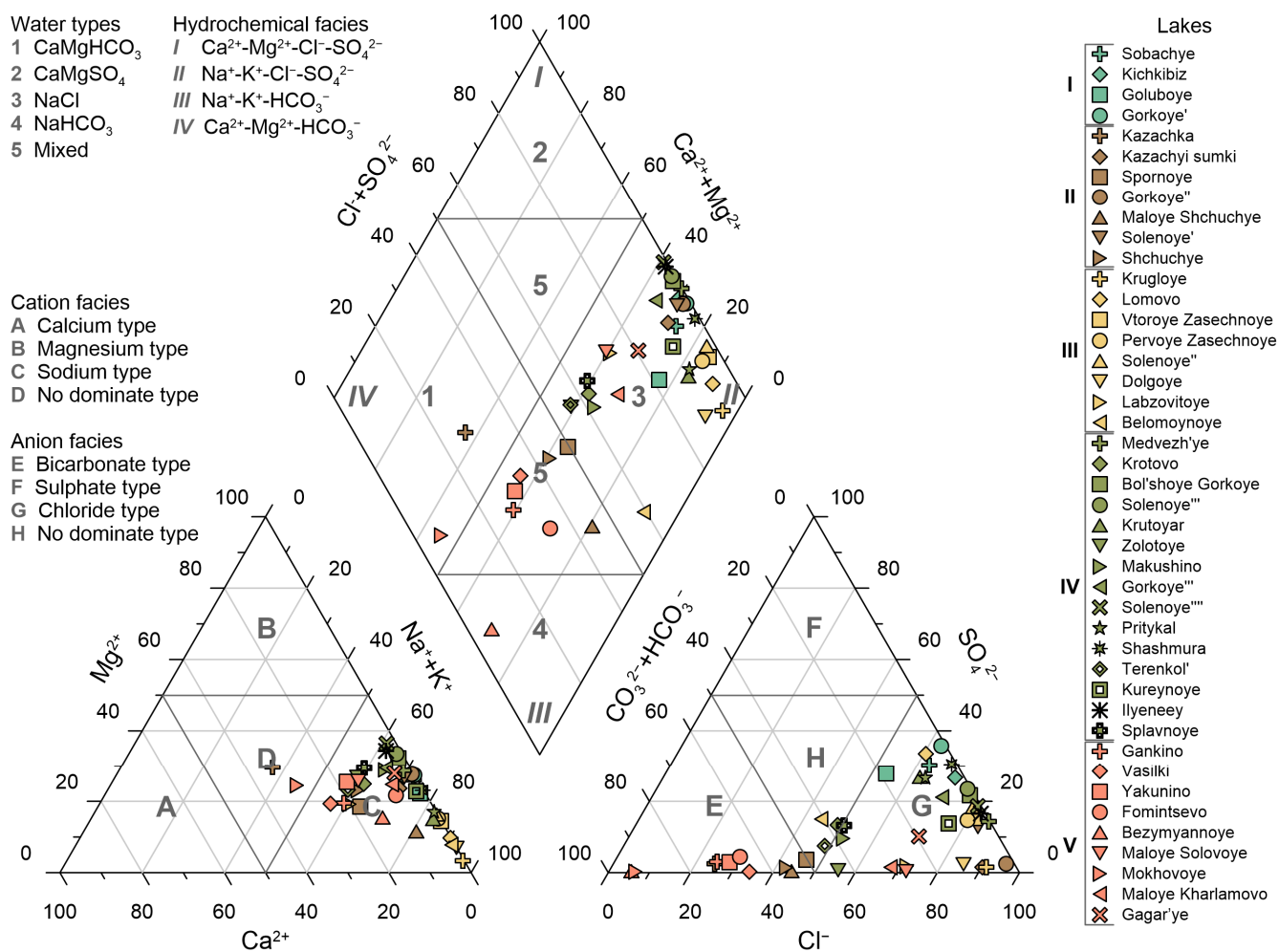


Figure 2. Piper diagram of the water chemical data from semiarid lakes in the southwest of Western Siberia. Groups of lakes denoted by color and roman numerals. Note that the DIC is represented by the sum of HCO_3^- and CO_3^{2-} ions.

The relationship between the morphometric characteristics of lakes and the physico-chemical parameters of the water column was assessed based on the analysis of Spearman correlation coefficients (Table A6). Statistically significant ($p < 0.05$) weak and moderate positive correlations ($0.36 < r < 0.52$) were revealed between the lake area and TDS and the concentration of main cations and anions. These relationships can be explained by different volumes of water evaporating from the surface of lakes having different size, which leads to uneven levels of seasonal concentration of solutes. Moreover, the different area of the water bodies controlled the potential role of groundwater and its connectivity to the water column of the lake. The contribution of precipitation and surface runoff depended on the watershed area. There were also weak but positive correlations between catchment area and major ion content ($0.4 < r < 0.5, p < 0.05$). At the same time, the average depth of water bodies did not control the water chemistry ($r < 0.3; p > 0.05$). A moderate inverse relationship was noted between pH values and Ca concentration in the lake water ($r = -0.53, p < 0.05$), which can be explained by the fact that dissolved Ca^{2+} ions are able to remove the excess of dissolved carbon dioxide, lowering the acidity of the waters [37]. The TDS values demonstrated strong link ($r > 0.9, p < 0.05$) with the concentration of Cl^- , Na^+ , Mg^{2+} , SO_4^{2-} , DOC and strong correlation ($r = 0.82, p < 0.05$) with the concentration of K^+ . The maximum r value was observed between Na^+ and Cl^- (0.98). It was previously shown that chlorides dominated the mineralization for the studied water bodies. Moderate positive correlations were noted between TDS with Ca^{2+} and DIC ($0.5 < r < 0.7$). Major cations and anions, DOC

and DIC are mutually correlated with each other at the $p < 0.05$ level. Additional regression analysis was carried out between the most important components of the carbon cycle in the lakes. The DOC was moderately correlated with Mg^{2+} ($r^2 = 0.59$, $p < 0.00001$). However, there was no linear relationship of DOC with Ca^{2+} ($r^2 = 0.002$, $p = 0.785$). The DIC was related to none of these inorganic components ($r^2 < 0.12$, $p > 0.02$), which likely stems from complex salt composition and the history of the formation of the studied lakes.

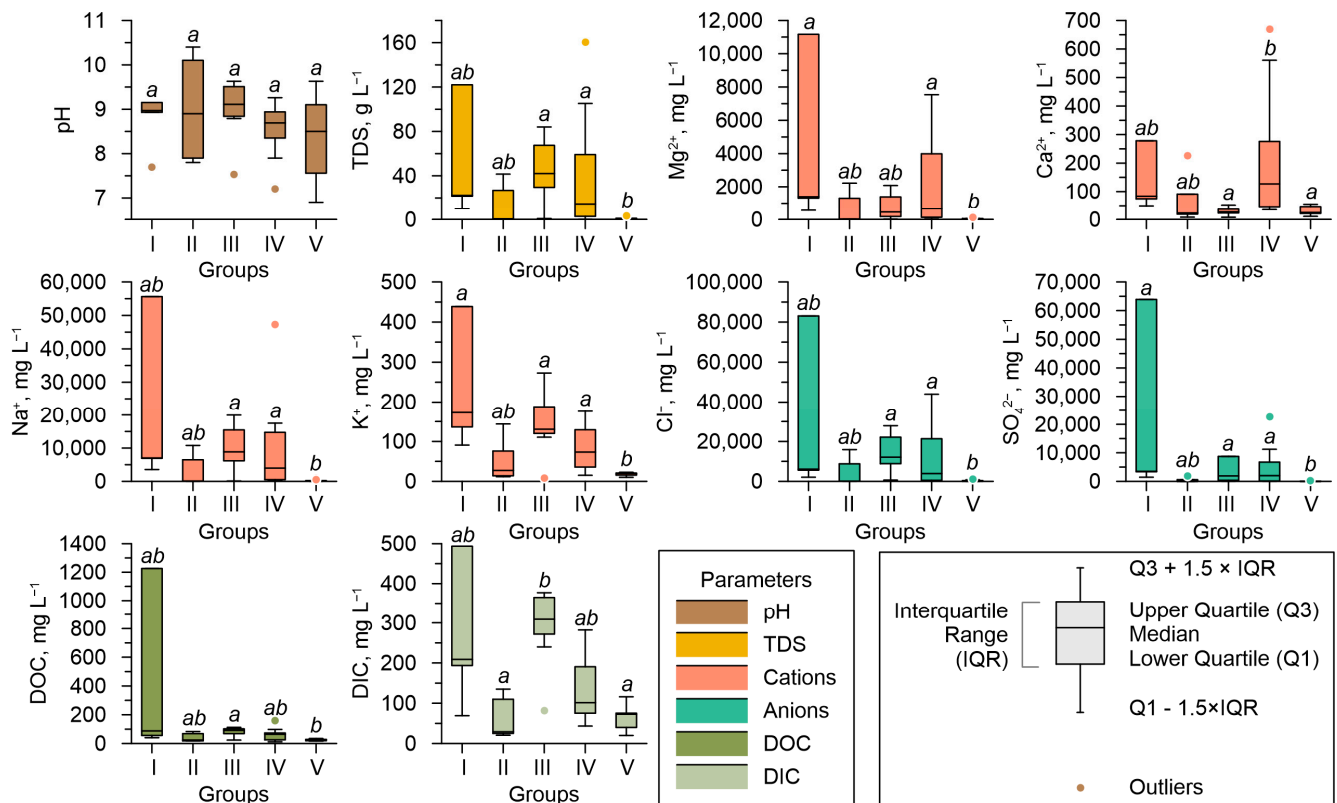


Figure 3. Variation in hydrochemical properties between groups of the semiarid lakes of the southwest of Western Siberia. Different letters indicate significant differences ($p < 0.05$) resulting from the multiple comparisons of p -values.

3.2. Water Chemistry as a Factor of Mineral Formation

The values of Mg/Ca molar ratio fluctuated over a wide range, from 0.8 to 198 for all of the studied water bodies. In 35% of the lakes, the Mg/Ca molar ratio was below 2. These lakes also demonstrated lower TDS values ($< 1 \text{ g L}^{-1}$). For 35% of the studied water bodies, the Mg/Ca molar ratio was above 10. These lakes were also characterized by elevated TDS values, though no pronounced relationships between this Mg/Ca molar ratio and TDS were observed (Figure 4). A regression analysis demonstrated that there are significant ($p < 0.05$) linear relationships between Mg/Ca molar ratio, TDS and DOC/DIC. At the same time, the identified relationships between mentioned parameters and Mg/Ca molar ratio were rather weak ($R^2 < 0.5$).

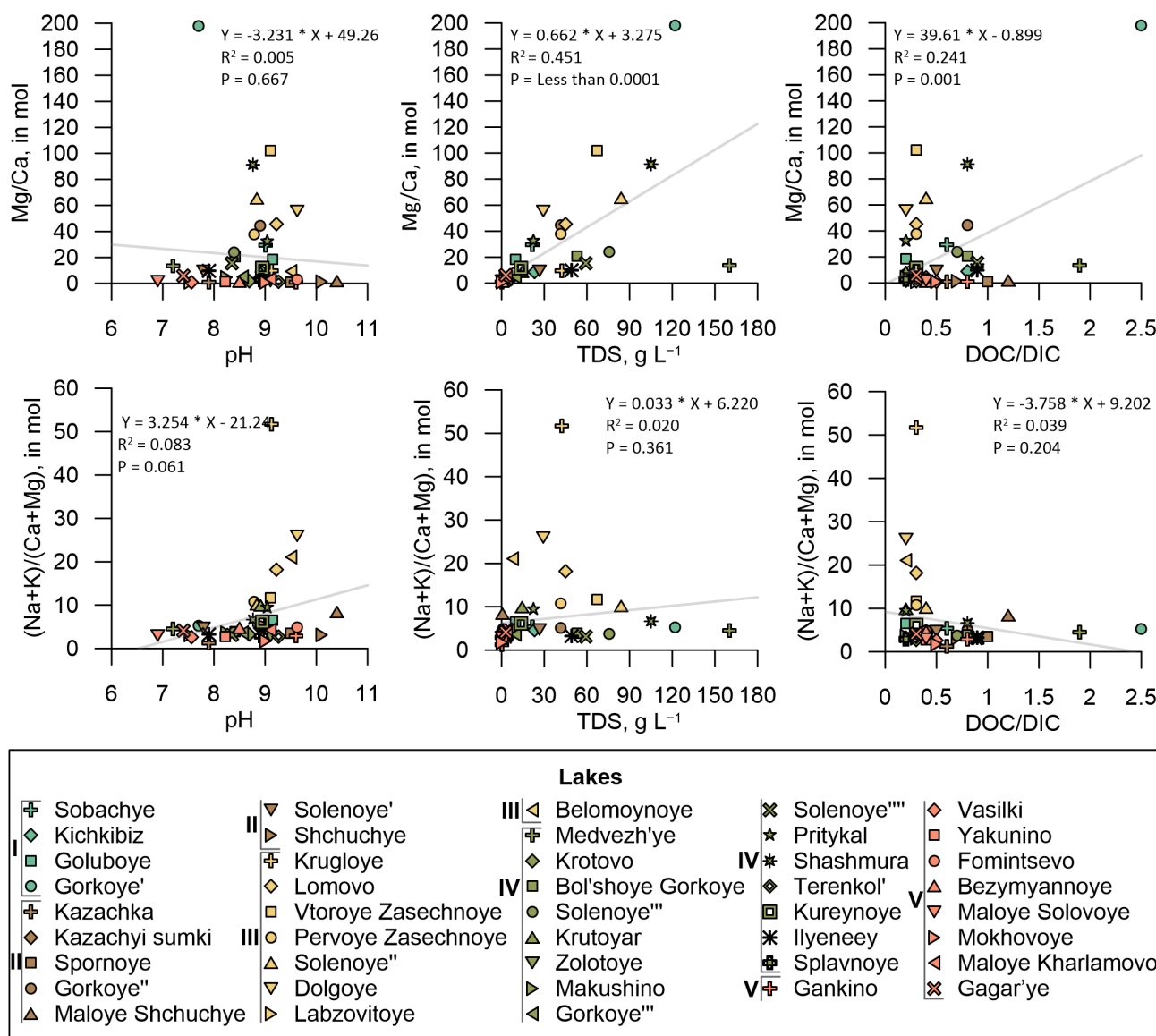


Figure 4. Mg/Ca and (Na+K)/(Ca+Mg) molar ratios plotted against pH, TDS, and DOC/DIC in water of the semiarid lakes of the southwest of Western Siberia. Groups of lakes denoted by color and roman numerals.

The (Na+K)/(Ca+Mg) molar ratio varied from 1.2 to 52 among all studied water bodies. At the same time, no statistically significant linear relationships between the values (Na+K)/(Ca+Mg) ratio and other hydrochemical parameters were observed (Figure 4).

Thermodynamic modelling of water–rock equilibrium performed using the Visual MINTEQ allowed to identify possible secondary carbonate minerals in the studied lakes of different types. Their water saturation indices (SI) are listed in Table A3 of the Appnedix. The saturation indices (SI) of minerals systematically changed depending on the pH and TDS values (Figure 5). According to the Visual MINTEQ results, as pH increases, carbonates have a possibility to precipitate in the following order: dolomite (CaMg(CO₃)₂, ordered and disordered), aragonite (CaCO₃), calcite (CaCO₃), vaterite (CaCO₃) at pH > 7.9; magnesite (MgCO₃), huntite (Mg₃Ca(CO₃)₄ at pH > 8.2; monohydrocalcite (CaCO₃·xH₂O) at pH > 8.9. Artinite (Mg₂CO₃(OH)₂·3H₂O) and hydromagnesite (Mg₅(CO₃)₄(OH)₂·4H₂O) could precipitate at pH 8.7–9.2. Regardless of the salinity in the solution, precipitation of dolomite (ordered and disordered), aragonite, calcite, vaterite is possible for all studied aquatic environments. At TDS > 1 g L⁻¹, the solutions become oversaturated, and magnesite and

huntite precipitation is also possible. Monohydrocalcite, artinite and hydromagnesite can precipitate in highly lakes with saline waters.

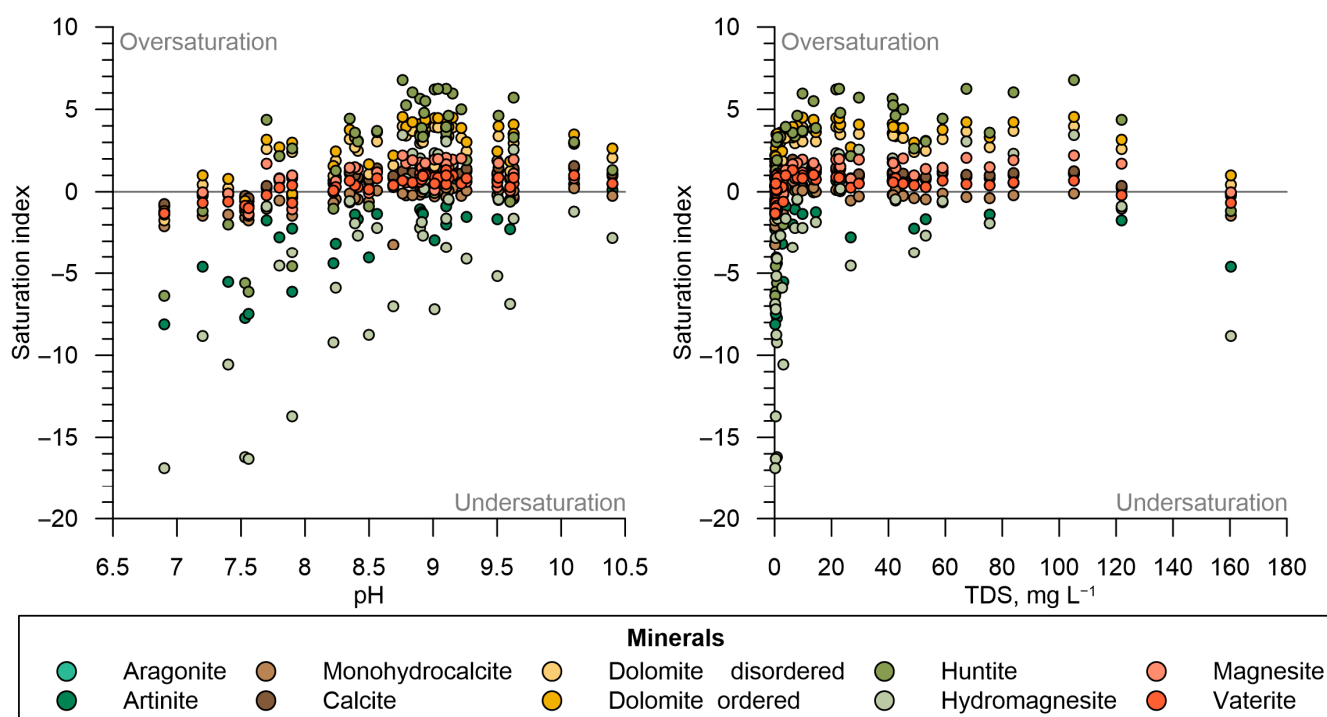


Figure 5. Saturation indices of carbonate minerals plotted versus pH and TDS values.

3.3. Lithology and the Bulk Mineralogical Composition of Sediments

In most cases, the upper layer of sediments was represented by a dark-grey organic-rich material, varying between different lakes depending on the proportion of mineral matter. According to the textural differentiation, the upper layer of sediments exhibited distinct granulometric composition (Figure 6). Sediments from lakes of I–III and V groups were characterized by a significant proportion of sand fraction, while the group IV lakes sediments referred to loams with a sizable proportion of silt fraction.

Based on the results of XRD and SEM-EDS analytical studies, we have identified terrigenous and authigenic minerals constituting the sediments of forest-steppe lakes of the southwest of Western Siberia (Table A4 of the Appendix A). For the majority of the studied aquatic environments, quartz and, to a lesser extent, feldspars prevailed among the terrigenous constituent with a small admixture of muscovite, biotite, accessory minerals and other aluminosilicates.

For most of the sediment samples, minerals from the group of clay aluminosilicates such as smectite-montmorillonite, illite and chlorite were identified. Clay minerals were identified in non-oriented samples by non-basal reflections $d/n \sim 4.45, 2.55 \text{ \AA}$. Illite basal reflections $\sim 10.1\text{--}10.4 \text{ \AA}$, smectite $d_{001} \sim 13.8\text{--}14.5 \text{ \AA}$, chlorite- $d_{001} \sim 14.2\text{--}15 \text{ \AA}$, mixed-layer phases were also present. According to the results of microscopic studies, there were clear signs of the authigenic formation of chlorite-hydromicaceous material in cavities and caverns of the substrate mass. This suggested the authigenic formation of clay minerals in lacustrine sediments, that can be intensified during the recent period as a result of enhanced erosion caused by agricultural activities within the watersheds as known in other desert and semi-desert settings [38].

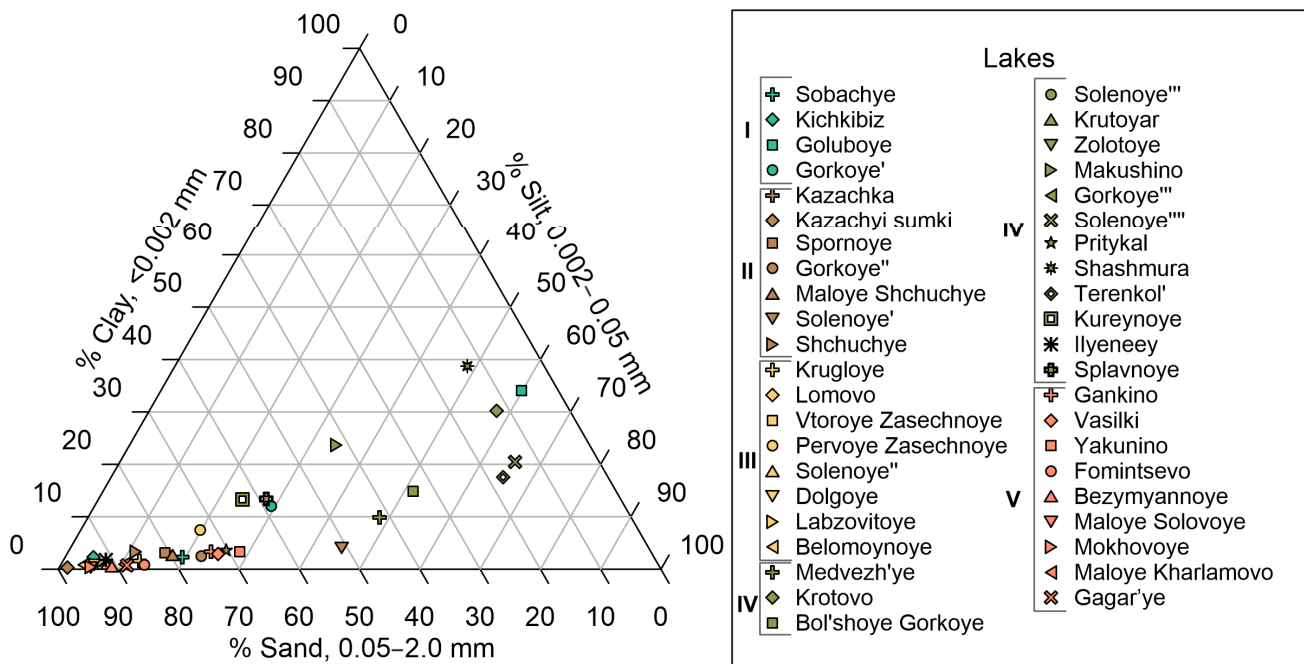


Figure 6. Sand-silt-clay values for 36 sediment samples plotted on the USDA textural triangle.

Single aggregates of oxides and hydroxides of iron are found in sediments in insignificant amounts, mainly presented in the form of films on the surface of terrigenous grains and aggregates of hydromicaceous material. It is possible that the authigenic formation of iron oxides within the mass of the studied sediments was associated with post-sedimentary replacement of organic matter in the form of finely dispersed detritus and organic films [39,40].

The group of sulfate minerals was mainly represented by gypsum, whose formation could be linked to intensive fluctuations of water level during the summer period. As a rule, sulfates within the studied bottom sediments were represented by both single elongated columnar and flat microcrystals and aggregates of various configurations, most often in the form of rounded acicular gypsum microconcretions. For some lakes with highly mineralized brines, aqueous magnesium and sodium sulfates were identified, represented mainly by bloedite ($\text{Na}_2\text{SO}_4 \times \text{MgSO}_4 \times 4\text{H}_2\text{O}$) in lakes of I group, as well as loeweite ($\text{Na}_4\text{Mg}_2(\text{SO}_4) \times 4.5\text{H}_2\text{O}$), also reported in other lakes of the region [41] and kieserite ($\text{MgSO}_4 \times \text{H}_2\text{O}$) in lakes of III group. Among the authigenic minerals of the halide group, we identified only halite (NaCl).

3.4. Abundance and Diversity of Carbonate Minerals in Bottom Sediments of the Studied Lakes

Among the variety of authigenic minerals in sediments of the studied water bodies, carbonates hold a specific place in the context of our research. This class of minerals is found in almost all water bodies (Table A4 of the Appendix A). The most common carbonates include calcite (CaCO_3), Mg-calcite (Ca,MgCO_3), aragonite (CaCO_3), Ca-dolomite ($\text{Ca,Mg}(\text{CO}_3)_2$) and hydromagnesite ($\text{Mg}_5(\text{CO}_3)_4(\text{OH})_2 \times 4\text{H}_2\text{O}$); and in rare cases, siderite (FeCO_3) and rhodochrosite (MnCO_3). The composition of carbonates is quite dynamic, diverse, and is largely determined by a combination of features of specific aquatic environment.

The XRD patterns of most widespread carbonates are present in Figure 7. Calcite is the most common carbonate mineral which is present in sediments of all studied groups of lakes. The highest abundance of this mineral was observed for IV and V groups of lakes. According to the results of SEM-EDS analysis, calcite often forms pelitomorphic nodules within the clayey masse or it appears as intergrowths of well-formed rhombic isometric microcrystals. Aragonite is a rather common component of bottom sediments enriched in

gastropod shells, as well as artemia cysts (most of the brine-type and highly mineralized lakes of I and III group and several eutrophic lakes of the II, IV and V groups).

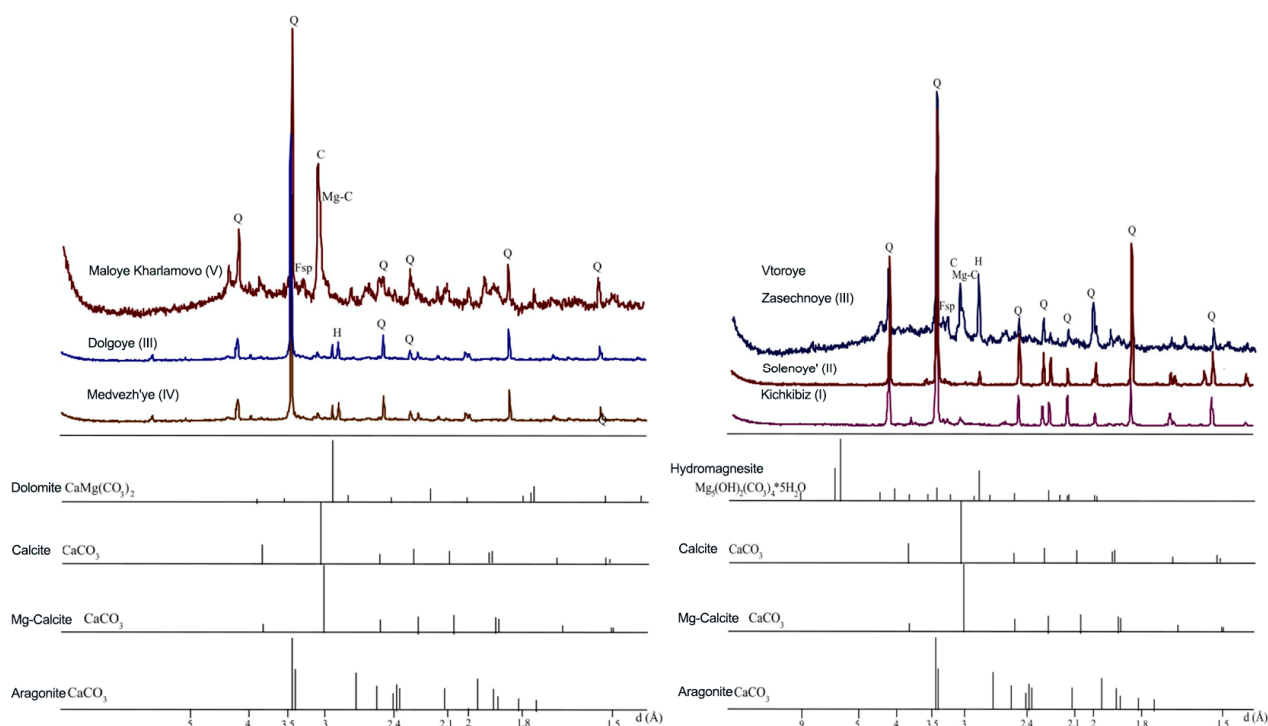


Figure 7. XRD patterns of most common carbonates recorded from lakes representing various groups.

For a large number of samples, the broadening of reflections suggests the presence of several calcite phases that differ in Mg content. According to the results of the XRD analysis, there was a continuous isomorphous miscibility for calcite-magnesite series with a corresponding change in the interplanar distances of minerals; therefore, the diffraction patterns of Mg-calcite differ from those of calcite. Mg-calcite is observed in variable amounts in sediments of all lakes. Basically, this mineral formed aggregates with hydromagnesite or proto-dolomite, most often it formed large communities of single elongated split sheaf-like microcrystals that develop within the EPS films, rarely forming rather large poorly cemented homogeneous nodules.

Dolomite appeared in sediments of III and IV group lakes in small amounts. Given intrinsic limitations on quantification of mineral proportion by the XRD analysis ($\pm 100\%$ for 2–3% of total fraction), we can only discuss the abundance of this component. At the same time, the SEM-EDS microanalyses have shown that this mineral appears as small inhomogeneous microcrystalline concretions, mainly in a mixture with high-magnesian calcite (Figure 8). In several cases there were dolomite microcrystals formed during the mineralization of EPS films in the form of single scattered cubic-like microcrystals. More rarely, dolomite appeared as large aggregates, consisting of co-directional columnar crystals with a high content of magnesium (17.6% mass fraction of Mg and 2.5% for Ca). In such cases, non-mineralized carbon-rich biogenic microfilms were observed on the surface of the aggregate and between individual columnar crystals, which is a commonly described pathway of Mg-rich carbonates precipitation in aquatic environments [42,43].

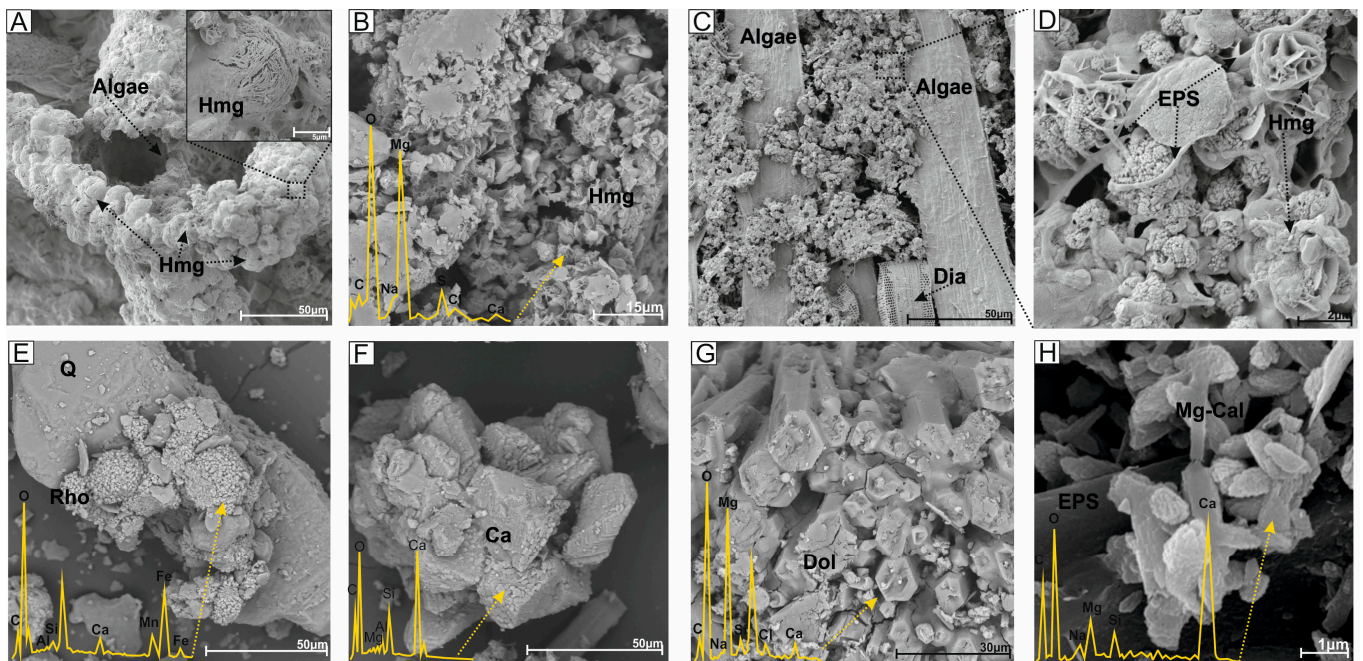


Figure 8. SEM images illustrating authigenic carbonates: (A) Mineralized algal filaments covered with a shell of spherical microaggregates of hydromagnesite (Lake Vtoroye Zasechnoye). (B) massive hydromagnesite aggregates (Lake Dolgoye). (C,D) Microaggregates of hydromagnesite formed on the surface of living algal filaments along EPS films (Lake Solenoye). (E) Spherical microaggregates of high-iron rhodochrosite on the surface of terrigenous quartz grains (Lake Kich-kibiz). (F) Intergrowths of microcrystals of authigenic calcite (Lake Kichkibiz). (G) Intergrowths of columnar (columnar) microcrystals of high magnesian dolomite (Lake Goluboye). (H) Split sheaf-shaped microcrystals of dolomite, formed on EPS films (Lake Medvezh'ye).

Hydromagnesite occurred in sediments of a number of water bodies from I, II and III groups. It was rather common for the lakes of the third group, where it was previously reported as characteristic mineral of near-shore facies and microbialites [26,41]. According to the results of SEM-EDS analysis, this mineral appeared as continuous zones of plate-like radially divergent crystals, associated in dumbbell or star-like clusters, that develop over extracellular polysaccharides (EPS) films. This form is rather common for this mineral, which often occurs in contemporary aquatic settings [44–47].

4. Discussion

4.1. Hydrochemical Features and Variability of Forest-Steppe Lakes in the Southwest of Western Siberia

While discussing the lakes in the southwest of Siberia, we noted that differences between neighboring groups are often less pronounced than the intergroup variability. The main tendencies are related to the changes in geographical context—first of all, to the distance from the Ural Mountains, which is pronounced as a decrease in TDS and the transformation of water type. The fact that the waters of the group V lakes are of the magnesium bicarbonate type, while all other groups correspond to the sodium chloride type, can be explained by the difference in geomorphological context. The V group lakes occur in the central part of the Ishim Plain at a significant distance from the large river valley. Such context predetermines thicker cover of late quaternary loess-like loams and high heterogeneity of covering deposits and, therefore, different hydrogeological conditions. Unlike the I-IV localities, salinization of soils is less common for the central part of the Ishim Plain in contrast with the Trans-Ural Plain [48].

The intergroup variability of main hydrological parameters for the studied lakes was rather high. In the case of groups I and III, this fact can be explained by the presence of

water bodies significantly different in terms of TDS, as well as adjacent lakes that can form gradients from mineralized to brine-type aquatic environments. In fact, the differences in TDS within one group of water bodies can exceed three orders of magnitude (Figure 3; Table A5 of the Appendix A). It is possible that such drastic differences stem from variable evaporation regime, leading to intensive temporal fluctuations of the water level and chemistry of the water column [49–52]. The presence of brine-type waters within the group I may also explain strong differences in the DOC and DIC concentrations.

The lakes of group II and V are characterized by stronger fluctuations in pH, probably related to macrophytes that overgrow the water reservoir as known in other settings [53]. Nevertheless, overall variability of pH values, both within each group and in the entire sample set, was low ($CV < 33\%$), which implies a homogeneity of acid-base conditions (Table A5). According to the Kruskal–Wallis and the median tests (Figure 3), there were no statistically significant differences between the groups of lakes in terms of the median pH value.

There are multiple reason of high intergroup hydrochemical variability of the studied forest-steppe water bodies. Each group is characterized by a similar morphology, genesis and general landscape context. The statistical treatment of the data revealed weak positive correlation between the surface area of the studied lakes and concentration of anions and cations (Table A6 of the Appendix A). Tentatively, this can be explained by the variations in water chemistry as a result of different degree of evaporation and groundwater influence. The more evident reason for high intergroup variability of water chemistry within the certain group is the context of late quaternary evolution of aquatic environments and adjacent area. The morphology of shoreline, as well as adjacent lake depression in most cases shows signs of strong long-term level fluctuations [54–56], leading to connectivity of water bodies through recently dry channels. After the isolation of single lakes, their further evolution could be controlled by different local erosional activity within the watershed and potential of evaporation which, in turn, are related to the morphology of specific depression.

When comparing the studied lakes with water bodies of other semiarid regions of Western Siberia, it is worth mentioning, that they were characterized by sodium chloride waters, and rarely by magnesium bicarbonate type, while within the Baraba lowland and Kulunda plain bicarbonate-sodium water composition was more common [7]. An increase in evaporation and a decrease in precipitation in the Central Eurasian region, including south of Western Siberia as a results of on-going climate warming will likely increase overall TDS and lead to preferential removal of CaCO_3 and, in a lesser degree, MgCO_3 -rich carbonates from the water column to the sediments. This may lead to further enrichment of the lake waters in Na, Cl, and SO_4 while impoverishing the waters in Ca, DIC and Mg. Such a transformation will certainly decrease the lake productivity, water quality and overall utility of the lakes for ecosystem services.

Another characteristic feature of the studied lakes is related to rather high DOC values. It is generally accepted that DOC values should decrease, while DIC increase across the aridization gradient. In our case the average DOC values for all mentioned water bodies reach 80 mg L^{-1} , which is comparable or higher than that in arctic and boreal thermokarst lakes of permafrost peatlands, Western Siberia [57] and higher than that in semiarid and arid lakes of Chinese regions [58,59]. On the other hand, similar to the Western Siberian forest-steppe lakes, high DOC values ($32\text{--}330 \text{ mg L}^{-1}$) are reported for the water bodies of Alberta, Canada [60]. In the case of Canada, this fact is explained by an increase in DOC concentration with an increase in water residence time, leading to sizable evapo-concentration with increasing salinity, while preserving the internal DOC sources [60,61]. Therefore, a high DOC level in the studied lakes of southwestern Siberia can be viewed as a typical feature of the transitional ecotone of steppe/forest-steppe, analogous to that in Northern America. Note that the bottom sediments of lakes within the Ishim Plain are represented by predominantly organic-rich sapropels [19,26].

4.2. Diversity and Factors of Carbonate Formation in Bottom Sediments of Lakes in the Southwest of Western Siberia

A high Mg/Ca ratio is considered among the most important factors of endogenous Mg-Ca and Mg-carbonate mineral formation [62–65], whereas high values of (Na+K)/(Ca+Mg) molar ratio are an indicator of calcite precipitation [17]. Figure 9 illustrates the interrelations between the Mg/Ca ratio and the predominant associations of carbonate minerals.

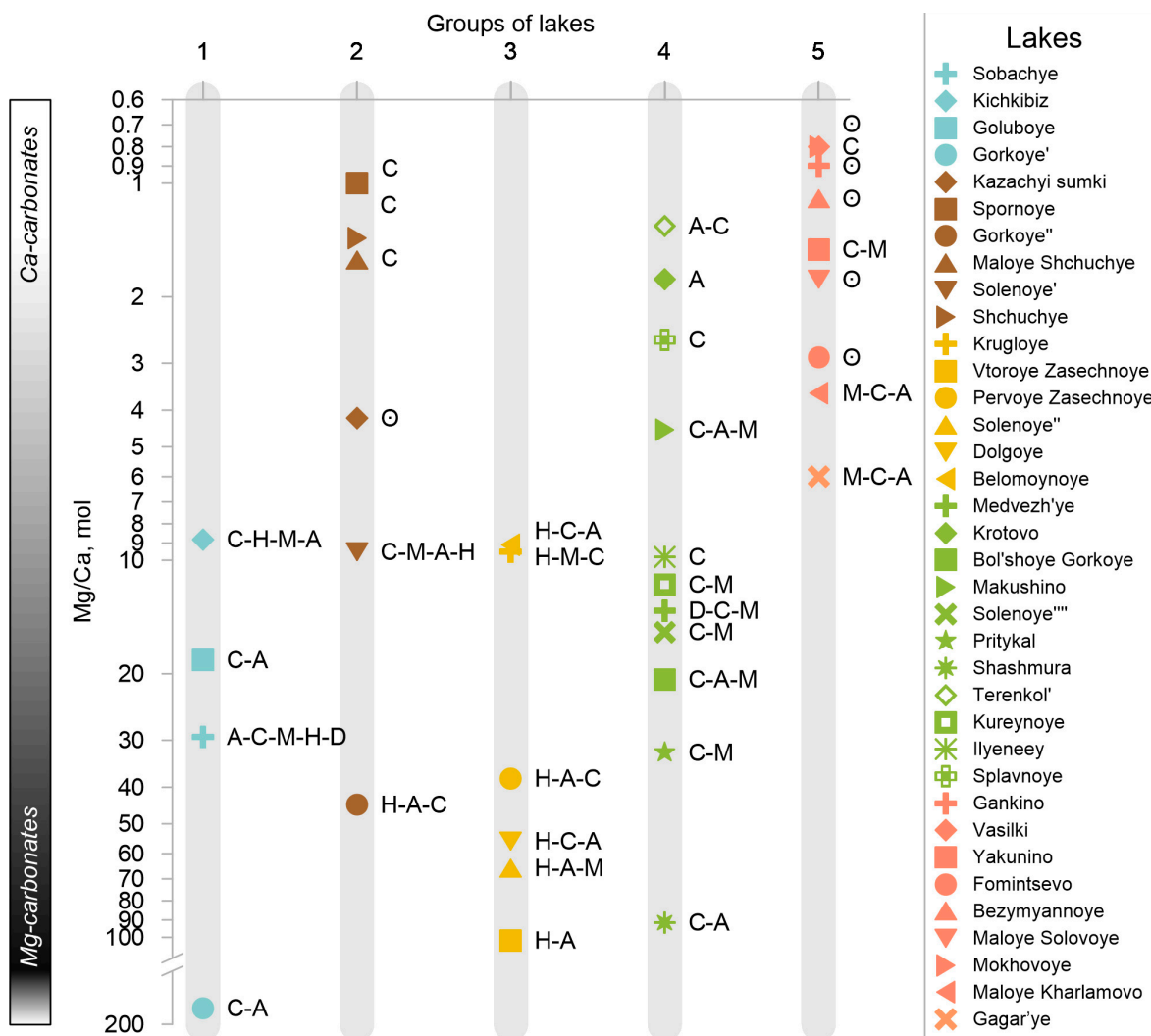


Figure 9. Relationship between Mg/Ca molar ratio in lake waters and authigenic carbonate mineralogy in sediments. Carbonates: C calcite, A aragonite, M Mg-calcite, D dolomite, G hydromagnesite, and O not found.

Thus, analyzing Figure 9, we can conclude that the authigenic carbonates in bottom sediments of the studied lakes are represented predominantly by Ca-carbonates with a Mg/Ca ratio in water below 32. Mg-Ca-carbonates appear at a Mg/Ca ratio ranging from 1.5 to 13.6, Mg-carbonates appear at an Mg/Ca of 9.5 and predominate in the composition at a Mg/Ca ratio between 44.5 and 102. The studied lakes meet all these criteria and hence are capable of precipitating various Ca, Mg carbonates in the water column and sediments. According to the results of thermodynamic assessment of SI (Figure 5; Table A3), not all of the above carbonates that could potentially precipitate in the studied aquatic environments were observed. At the same time, the results of XRD analysis for all studied lakes (Table A4 of the Appendix A), as well as hydrochemical studies (Table A2), make it possible to assess the influence of various factors on the occurrence of most common carbonates.

Thus, aragonite is present in bottom sediments containing gastropod shells of antheia cists, which are abundant in bottom sediments of some water bodies (all lakes of the I and III groups and certain water bodies from other groups). This may reflect some dependence of the degree eutrophication (or simply overgrowth by macrophytes) of lakes and the amount of aragonite in bottom sediment samples. Overall, observations on aragonite occurrences in the studied lakes corroborate the importance of aragonite in mineralization of skeletal structures reported in former studies [66,67].

Calcite is found almost everywhere; its content varies significantly depending on the composition of the waters and the granulometric composition of bottom sediments. Hydromagnesite is typical only for a number of water bodies of I and III groups with very high Mg/Ca ratios. The localization and the morphology of aggregates in general was rather similar to other reported case of modern hydromagnesite within the aquatic environments of mineralized lakes and lagoons [68–72]. The hydromagnesite observed in the studied water bodies is often associated with biogenic processes, as well as for a number of reported cases [73–75]. Dolomite, which is formed in some reservoirs of III and IV key areas, is mostly observed using SEM, since it is not always identified on X-ray diffraction analysis due to its low content. Mg-calcite is observed in varying amounts in water bodies of all key areas. This mineral mainly forms aggregates with hydromagnesite or dolomite, and presents as large communities of single elongated split sheaf-like microcrystals. These crystals likely occur within EPS films produced by bottom microbial consortia, and therefore rarely forms as large poorly cemented homogeneous nodules.

Note that in this work, we could not assess the impact of anthropogenic activity on lake hydrochemistry and the carbon cycle. In fact, such a study would require a comprehensive analysis of major nutrients (N, P) in the water column and incoming streams. We would expect here that different forms of dissolved nitrogen originated from fertilizers or sewage would not directly impact carbonate mineral formation, other than increasing the frequency of bloom or coastal biofilm growth. In contrast, excess phosphate delivery from the watershed may not only boost the algal activity, but directly inhibit CaCO_3 precipitation in the water column, while affecting hydrous MgCO_3 precipitation in a lesser degree.

In general, our study demonstrate that Mg-carbonate formation is potentially important for assessment of carbon sequestration within the studied aquatic environments, given that this process was reported for at least two groups of lakes present in this study. Taking into account the fact that Mg-carbonates were also reported for a number of other lakes of south Siberia and Central Eurasia by D.S Shlyapnikov [26], we can suggest that the process of their formation is not a very rare case for the studied part of Western Siberia. Unlike the Baraba and Kulunda regions where precipitation of Mg-Ca and Ca carbonates was predominant [7,76,77], in our study the Mg-carbonates significantly contributed to the authigenic mineral formation. Therefore, estimation of the C burial flux related to this process, understanding the relative role of biotic and abiotic controls, paleo-limnological aspect, as well as modern abundance of Mg-rich carbonate should be the priority of more comprehensive studies. These should allow enable estimation of the potential of southwestern West Siberian water bodies, including saline lakes, in C storage and inorganic C burial under the natural and anthropogenically induced transformation of climate and landscapes [78].

5. Conclusions

The present study reports new data on the hydrochemistry of the water column and bottom sediments mineralogy of drainless lakes in southwestern Siberia in relation to the inorganic C cycle and CO_2 uptake/release by these lakes. Three main conclusions are drawn:

- Lake waters exhibited significant differences in hydrochemistry, with sizable heterogeneity among groups of lakes and among water bodies within each group. Most lakes have weakly alkaline to strongly alkaline waters and are of the saline or brine type. A weak correlation was found between the morphology of lakes and the composition of

waters. According to the composition of major solutes, most lakes are of the sodium-potassium chloride-sulfate salt type. The lakes of the eastern V group, confined to the Ishim Plain, are distinguished by the highest content of organic matter in bottom sediments and sizable amount of aquatic plants (macrophytes) in the coastal zones. The water bodies of the III group are characterized by the highest content of DOC and the lowest Ca concentrations in the water column. The lakes of the third group are distinguished from the other groups by the highest values of the Mg/Ca ratio. Overall, high DOC concentrations are characteristic for all studied groups of lakes.

- The mineral composition of lake sediments, as determined by XRD and SEM-EDS analyses, demonstrated that the bulk of sediments is represented by a terrigenous component, consisting mainly of quartz and feldspars. Among authigenic minerals, minerals of the carbonate class are most common, and to a lesser extent, halides, sulfates, sulfides, oxides, and hydroxides. Heterogeneity of the mineral composition, primarily in terms of authigenic minerals, was observed both between groups, and within certain water bodies. Alkaline-earth carbonates are the most common class of authigenic minerals and include calcite, Mg-calcite, aragonite, Ca-dolomite and hydromagnesite, as well as siderite and rhodochrosite in some cases.
- Water bodies of the group III with highest Mg/Ca molar ratios are characterized by the greatest variety of magnesium minerals, primarily magnesium carbonates, and also have abundant signs of biomineralization, whereas bottom sediments of the group V are distinguished by the presence of iron oxides, which, apparently, can be explained by the lithology and the nature of land use of adjacent agricultural areas within the lake watershed. Overall, the observed differences in the composition of the authigenic part of the mineral component of sediments may stem from a combination of factors, including, but not limited to, the degree of their eutrophication, the intensity of the erosion and agricultural activity within the watershed.
- The main limitation of the present study is its low seasonal resolution (lack of spring, autumn and winter measurements) when extensive exchange of CO₂ with atmosphere could occur, as known from works on other regions in Siberia [79]. The obtained results, however, encompass the most active open water period and, as such, can be considered as representative for assessing atmospheric C sequestration potential in bottom sediments. Missing in these evaluations is organic C burial [80], which should be a focus of further research.

Author Contributions: Conceptualization, A.K. (Alexandr Konstantinov) and O.S.P.; methodology, A.N., A.K. (Alexandr Konstantinov) and O.S.P.; validation, A.K. (Alexandr Konstantinov) and E.K.; formal analysis, A.N. and E.K.; investigation, A.N., A.K. (Alexandr Konstantinov), E.K., Y.S., A.L. and A.K. (Alina Kurasova); resources, S.L.; data curation, A.N. and E.K.; writing—original draft preparation, A.N., A.K. (Alexandr Konstantinov) and E.K.; writing—review and editing, A.K. (Alexandr Konstantinov), E.K. and O.S.P.; visualization, A.N., E.K. and Y.S.; supervision, A.K. (Alexandr Konstantinov) and O.S.P.; project administration, A.K. (Alexandr Konstantinov); funding acquisition, O.S.P. All authors have read and agreed to the published version of the manuscript.

Funding: O.S.P. is grateful for support from the TSU Development Programme PRIORITY—2030 and ANR MeLiCa.

Data Availability Statement: Data are openly available within this article in Appendix A.

Conflicts of Interest: The authors declare no conflict of interest.

Appendix A

Table A1. Location and morphological parameters of the studied lakes.

Lake	Group	Coordinates		Area, km ²	Watershed, km ²	Average Depth, m
Sobachye	I	54°22'4.97"	61°40'42.01"	0.45	1.57	1.8
Kichkibiz	I	54°20'6.12"	61°40'25.07"	5.96	12.4	2.5
Goluboye	I	54°20'1.73"	61°45'0.36"	1.4	2.9	2
Gorkoye'	I	54°19'22.49"	61°43'4.73"	3.63	5.9	1.5
Kazachka	II	54°16'59.34"	62°31'7.55"	0.46	1.37	1.8
Kazachyi Sumki	II	54°18'8.61"	62°31'8.11"	0.65	1.12	1.6
Spornoye	II	54°19'56.78"	62°28'53.81"	0.41	0.75	1.3
Gorkoye"	II	54°18'29.04"	62°27'57.05"	1	1.66	1.3
Maloye Shchuchye	II	54°19'27.95"	62°27'27.52"	0.4	0.92	1.6
Solenoye'	II	54°18'34.18"	62°25'45.19"	0.27	0.6	1.4
Shchuchye	II	54°19'48.53"	62°26'5.51"	0.5	0.87	1.5
Krugloye	III	54°37'40.93"	64°1'42.36"	1.27	2.62	1.5
Lomovo	III	54°37'40.93"	64°1'42.36"	0.67	1.67	1.4
Vtoroye Zasechnoye	III	54°37'42.85"	64°0'49.08"	1.68	3.62	2
Pervoye Zasechnoye	III	54°37'40.93"	64°1'42.36"	1.39	3.14	1.1
Solenoye"	III	54°37'40.93"	64°1'42.36"	1.11	2.44	2.3
Dolgoye	III	54°38'27.99"	64°1'33.74"	1.7	4.51	1.8
Labzovitoye	III	54°39'29.48"	63°55'28.94"	0.22	0.4	1.7
Belomoynoye	III	54°39'34.36"	63°53'21.08"	1.25	1.97	1.5
Medvezh'ye	IV	55°11'30.70"	67°57'5.77"	67.3	161	0.6
Krotovo	IV	55°11'37.68"	66°54'48.40"	0.54	1.51	1.1
Bol'shoye Gorkoye	IV	55°11'58.91"	66°53'23.57"	3.12	5.31	1.2
Solenoye""	IV	55°8'52.62"	66°54'47.29"	7.25	12.9	1.6
Krutoyar	IV	55°9'49.59"	66°57'25.61"	0.47	0.78	1.4
Zolotoye	IV	55°6'43.99"	66°58'42.62"	1.08	2.44	2.3
Makushino	IV	55°12'0.01"	67°14'7.10"	2.45	4.21	1.8
Gorkoye""	IV	55°4'40.25"	67°1'39.21"	0.86	1.4	1.7
Solenoye""	IV	55°2'53.15"	66°59'17.40"	0.83	1.35	1.5
Pritykal	IV	54°58'26.95"	66°58'39.04"	0.44	0.63	1.6
Shashmura	IV	54°57'10.48"	66°58'9.67"	0.62	0.95	1.1
Terenkol'	IV	54°55'18.74"	66°56'40.71"	2.7	4.2	1.2
Kureynoye	IV	54°54'29.73"	66°57'13.31"	3.12	5.73	1.3
Ilyeneey	IV	55°2'35.91"	66°55'36.77"	3.57	5.47	1.3
Splavnoye	IV	66°55'36.77"	66°58'57.44"	1.67	3.32	1.2
Gankino	V	55°49'27.39"	67°58'25.80"	0.37	0.72	1.6
Vasilki	V	55°48'48.33"	67°58'23.01"	0.42	0.68	1.5
Yakunino	V	55°47'47.18"	68°0'48.97"	0.75	1.25	2
Fomintsevo	V	55°56'26.29"	67°52'49.61"	1.37	2.01	2.1
Bezymyannoye	V	55°56'47.33"	67°55'7.17"	0.33	1.13	1.9
Maloye Solovoye	V	55°56'49.92"	67°59'45.33"	2.21	3.66	3
Mokhovoye	V	55°55'32.18"	68°0'9.00"	0.32	0.55	2.5
Maloye Kharlamovo	V	55°54'2.02"	67°43'12.71"	1.43	2	3.1
Gagar'ye	V	55°56'43.00"	67°45'41.41"	0.38	1.1	1.6

Table A2. Physical and hydrochemical parameters of the studied lakes.

Lake	Date of Sampling	T, °C	pH	TDS	Mg ²⁺	Ca ²⁺	Na ⁺	K ⁺	Cl ⁻	SO ₄ ²⁻	DOC	DIC	Mg/Ca	(Na+K)/(Ca+Mg)
				g L ⁻¹	mg L ⁻¹									mol
Sobachye	08.08.2019	22.3	9.01	21.6	1323.92	74.22	6915.42	209.19	5607.41	3630.65	119.03	193.7	29.4	5.4
Kichkibiz	08.08.2019	20.8	8.93	23.0	1483.75	278.22	7150.81	136.4	6613	3359	56	69	8.8	4.6
Goluboye	08.08.2019	18.7	9.15	9.84	555.71	49.68	3557.47	90.84	2060	1452.1	40.28	224.09	18.4	6.5
Gorkoye'	09.08.2019	23.1	7.7	122	11,165.43	92.98	55,617.87	438.69	83,090.75	63,892.74	1226	493.58	198	5.3
Kazachka	04.08.2019	20.8	7.9	0.33	12.04	22.48	20.05	13.89	28.26	3.78	18.25	29.1	0.9	1.2
Kazachyi sumki	04.08.2019	20.2	8.9	7.07	233.39	91.01	1300.4	37.75	2266.02	50.11	25.31	67.75	4.2	4.8
Spornoye	05.08.2019	20.5	9.5	0.49	11.71	18.42	59.98	27.25	77.43	8	24.23	24.97	1	3.5
Gorkoye''	05.08.2019	24.8	8.9	41.5	2217.79	82.13	10,786.64	143.77	15,898.1	557.29	83.56	110	44.5	5.1
Maloye Shchuchye	05.08.2019	21.6	10.4	0.47	7.34	7.78	89.32	11.55	75.97	1	23.77	20.48	1.6	8.4
Solenoye'	06.08.2019	23.9	7.8	26.7	1308.08	226.26	6469.91	75.82	8784.08	1823.24	68.24	135.09	9.5	4.8
Shchuchye	06.08.2019	23.8	10.1	0.53	19.05	21.75	87	14.34	86.35	3.7	18.28	27.43	1.4	3.1
Krugloye	28.09.2018	22.3	9.12	42.4	170.49	29.71	9126.53	157.9	13,568.32	308.93	112.08	343.07	9.5	51.7
Lomovo	28.09.2018	12.1	9.22	45.1	642.59	23.28	11,225.81	139.1	11,630.54	8731.11	102	364.91	45.5	18.2
Vtoroye Zasechnoye	28.09.2018	24.3	9.1	67.4	1391.16	22.48	15,466.77	188.31	22,136	5645	95	275	102	11.7
Pervoye Zasechnoye	29.09.2018	23	8.79	41.6	826.78	35.94	8629.57	110.53	12,605.69	3132.77	68.82	271.67	37.9	10.8
Solenoye''	29.09.2018	24.9	8.84	84	2076.81	52.27	19,954.63	272.92	27,896	8754	100	240	65.5	10.1
Dolgoye	30.09.2018	21	9.63	29.5	248.72	7.38	6167.87	119.98	8809.44	330.4	88.42	354.62	55.6	26.0
Labzovitoye	30.09.2018	9.6	7.53	0.75	17.14	29.54	98.41	7.53	597.48	19.77	23.52	81.08	1	3.1
Belomoynoye	30.09.2018	12.7	9.51	8.01	82.74	15.03	1761.57	121.95	1390.12	642.22	57.4	377.16	9.1	21.1
Medvezh'ye	07.08.2018	23.4	7.2	160	3851.12	467.92	17,505.08	50.95	44,010.86	10,014	97.8	52.26	13.6	4.5
Krotovo	07.08.2018	13.4	8.69	0.15	47.64	43.18	213.45	15.02	215.07	79.1	11.86	54.8	1.8	3.2
Bol'shoye Gorkoye	07.08.2018	13.6	8.41	53.1	2532.57	201.84	9751.27	88.91	17,768.63	6751.59	71.04	93.72	20.7	3.9
Solenoye'''	07.08.2018	14.2	8.39	75.6	4018.55	276.04	14,721.92	73.16	26,705.89	11,233	73.44	101.28	2	3.7
Krutoyar	07.08.2018	15.0	8.91	14.5	283.55	54.39	2933.92	37.51	3439.42	2002.95	47.06	195.23	8.6	9.9
Zolotoye	18.03.2019	0.9	9.1	6.4	144.75	126.75	524.55	129.17	742.61	13.27	73.48	190.57	1.9	2.9
Makushino	07.08.2019	18	8.24	2.7	127.78	46.71	511.15	46.15	506.49	124.78	25.42	125.12	4.5	3.6
Gorkoye''''	07.08.2019	21.6	8.56	9.86	500.42	163.92	2047.64	35.59	2677.86	1086.42	26.12	103.09	5	3.6
Solenoye''''	07.08.2019	22	8.35	59.1	5268.86	560.52	16,660.18	87.7	21,319.44	6668.22	64.35	75.17	15.5	3.1
Pritykal	07.08.2019	22	9.04	22.6	889.74	45.22	8138.55	92.95	5890.3	3320.28	69.83	282.22	32.4	9.4
Shashmura	07.08.2019	22.5	8.76	105	7538.47	136.03	47,308.13	176.2	37,500.75	22,717.09	160.34	211.21	91.4	6.6
Terenkol'	08.08.2019	20.3	9.26	0.7	26.62	34.53	112.64	22.97	155.7	32.18	12.37	43.29	1.3	2.8
Kureynoye	08.08.2019	20.5	8.94	13.7	649.15	92.04	3980.9	129.14	3911.3	960.93	50.99	172.97	11.6	6.1
Ilyeneey	08.08.2019	20	7.9	49.1	3988.41	668.58	13,587.42	161.31	17,750.18	4837.43	70.66	77.74	9.8	3.3
Splavnoye	09.08.2019	19.9	8.92	2.1	97	61.55	353.45	25.86	404.79	141.96	20.99	93.8	2.6	2.9
Gankino	01.08.2019	16.7	9.6	0.25	5.87	10.33	25.91	13.05	23.34	4.01	16.19	19.97	0.9	2.9
Vasilki	01.08.2019	16.8	7.56	0.44	11.4	23.76	51.36	19.34	53.06	0.32	18.85	36.82	0.8	2.6
Yakunino	01.08.2019	17.6	8.22	0.83	30.01	34.12	117.16	17.47	89.55	12.29	26.94	75.27	1.5	2.7
Fomitsevo	02.08.2019	19.9	9.63	0.97	28.65	16.1	167.54	15.61	116.04	22.9	28.48	73.11	2.9	4.9
Bezmyannoye	03.08.2019	19.4	8.5	0.58	14.15	20.77	116.02	9.91	12.31	1.41	28.64	72.75	1.1	4.8
Maloye Solovoye	03.08.2019	18.4	6.9	0.11	50.05	46.87	207.51	20.72	347.28	2.41	20.7	57.79	1.8	3.0
Mokhovoye	03.08.2019	18.5	9.01	0.34	11.82	24.09	28.09	22.53	8.58	0.29	18.61	39.91	0.8	1.7
Maloye Kharlamovo	03.08.2019	18.0	9.1	3.83	113.96	52.38	585.71	19.34	729.73	21.88	32.41	105.23	3.6	4.3
Gagar'ye	04.08.2019	17.6	7.4	3.07	200.98	55.45	905.60	22.11	1142.97	224.32	34.38	116.01	6.0	4.1

Table A3. Saturation indices for selected minerals, calculated with Visual MINTEQ for the studied lakes.

Lake	Arg	Art	MHC	C	DD	OD	H	HM	M	V
Sobachye	1.305	0.689	0.105	1.450	3.932	4.493	6.224	2.337	1.973	0.877
Kichkibiz	1.380	0.030	0.180	1.520	3.500	4.070	4.800	0.180	1.520	0.950
Goluboye	1.422	0.385	0.225	1.570	3.921	4.497	5.982	1.675	1.968	0.987
Gorkoye'	0.216	-1.735	-1.007	0.361	2.592	3.150	4.376	-0.871	1.695	-0.211
Kazachka	-0.243	-6.117	-1.438	-0.096	-0.704	-0.136	-4.577	-13.719	-1.064	-0.674
Kazachyi sumki	1.262	-1.049	0.066	1.409	2.951	3.521	3.382	-2.198	1.107	0.830
Spornoye	0.997	-1.656	-0.198	1.144	1.893	2.462	0.736	-5.184	0.303	0.565
Gorkoye''	1.044	0.708	-0.156	1.188	3.566	4.117	5.632	2.022	1.785	0.621
Maloye Shchuchye	0.952	0.106	-0.243	1.098	2.059	2.623	1.315	-2.798	0.477	0.522
Solenoye'	0.673	-2.756	-0.526	0.817	2.166	2.721	2.180	-4.521	0.786	0.248
Shchuchye	1.409	0.457	0.216	1.553	2.932	3.487	3.006	-1.213	0.819	0.984
Krugloye	1.263	-0.534	0.063	1.409	3.373	3.934	4.631	-0.439	1.456	0.835
Lomovo	0.958	-0.194	-0.238	1.111	3.261	3.866	4.996	0.575	2.015	0.509
Vtoroye Zasechnoye	0.906	0.989	-0.297	1.050	3.676	4.229	6.241	3.047	2.049	0.482
Pervoye Zasechnoye	0.987	-0.195	-0.213	1.132	3.398	3.956	5.254	0.799	1.734	0.560
Solenoye'''	1.006	0.544	-0.198	1.150	3.681	4.231	6.051	2.310	1.934	0.584
Dolgoye	0.938	1.050	-0.261	1.085	3.514	4.080	5.712	2.553	1.966	0.508
Labzovitoye	-0.384	-7.731	-1.566	-0.228	-1.173	-0.557	-5.598	-16.202	-0.983	-0.837
Belomoynoye	1.308	-0.487	0.118	1.461	3.373	3.975	4.622	-0.437	1.753	0.861
Medvezh'ye	-0.242	-4.596	-1.451	-0.097	-0.438	0.995	-1.170	-8.806	-0.010	-0.668
Krotovo	0.830	-3.207	-3.207	0.983	1.611	2.210	0.286	-7.014	0.443	0.385
Bol'shoye Gorkoye	0.754	-1.660	-0.446	0.906	2.481	3.079	3.046	-2.640	1.382	0.308
Solenoye''''	0.836	-1.384	-0.367	0.988	2.714	3.309	3.574	-1.922	1.510	0.392
Krutoyar	1.189	-1.234	-0.005	1.340	3.049	3.641	3.867	-1.823	1.463	0.747
Zolotoye	1.796	-1.978	0.642	1.958	3.304	3.960	3.595	-3.413	1.672	1.323
Makushino	0.730	-3.157	-0.465	0.879	1.893	2.472	1.288	-5.866	0.657	0.293
Gorkoye''''	1.265	-1.334	0.069	1.412	3.060	3.624	3.692	-2.176	1.164	0.836
Solenoye''''	1.120	-0.625	-0.087	1.266	3.217	3.779	4.451	-0.575	1.453	0.691
Pritykal	1.278	0.563	0.079	1.424	3.922	4.484	6.250	2.263	2.000	0.850
Shashmura	1.115	1.067	-0.101	1.261	3.993	4.553	6.785	3.447	2.217	0.688

Table A3. Cont.

Lake	Arg	Art	MHC	C	DD	OD	H	HM	M	V
Terenkol'	1.259	−1.525	0.064	1.407	2.466	3.036	1.932	−4.120	0.621	0.828
Kureynoye	1.455	−0.031	0.258	1.602	3.793	4.361	5.518	0.761	1.745	1.024
Ilyeneey	0.833	−2.238	−0.373	0.980	2.417	2.988	2.640	−3.710	1.009	0.400
Splavnoye	1.393	−1.342	0.198	1.541	3.029	3.600	3.356	−2.647	1.064	0.960
Gankino	0.739	−2.278	−0.455	0.889	1.267	1.851	−0.597	−6.880	0.069	0.300
Vasilki	−0.549	−7.464	−1.743	−0.399	−1.435	−0.851	−6.127	−16.309	−1.349	−0.988
Yakunino	0.519	−4.400	−0.676	0.668	0.983	1.564	−1.014	−9.200	−0.027	0.081
Fomintsevo	1.278	−0.415	0.083	1.425	2.941	3.512	3.322	−1.638	1.091	0.845
Bezmyannoeye	0.598	−4.029	−0.597	0.746	1.089	1.662	−0.872	−8.767	−0.064	0.165
Maloye Solovoye	−0.875	−8.124	−2.070	−0.726	−1.728	−1.151	−6.368	−16.885	−1.373	−1.311
Mokhovoye	0.924	−2.943	−0.270	1.073	1.574	2.151	−0.060	−7.195	0.127	0.489
Maloye Kharlamovo	1.453	−0.862	0.258	1.602	3.265	3.844	3.959	−1.623	1.307	1.016
Gagar'ye	−0.163	−5.510	−1.359	−0.014	0.212	0.793	−1.964	−10.578	−0.116	−0.601

Notes: Arg Aragonite, Art Artinite, MHC Monohydrocalcite, C Calcite, DD Disordered dolomite, OD ordered dolomite, H Huntite, HM Hydromagnesite, M Magnesite, and V Vaterite.

Table A4. Mineralogical composition (%) of surface sediments of the studied lakes.

Lake	Quartz	Calcite	Mg-Calcite	Feldspar	Gypsum	Aragonite	Dolomite	Illite	Hydromagnesite	Siderite	Goethite	Halite
Sobachye	62.2	2.9	2	14.3	−	4.8	0.8	10.9	1.1	−	−	1
Kichkibiz	76	6.0	2.2	2.2	3.3	2	−	4.3	3.8	−	−	0.2
Goluboye	76.9	7.1	−	12.7	−	3.3	−	−	−	−	−	−
Gorkoye'	74.8	3.1	−	18.4	2.7	1	−	−	−	−	−	−
Kazachyi sumki	97.3	−	−	2.7	−	−	−	−	−	−	−	−
Spornoye	92.4	0.5	−	7.1	−	−	−	−	−	−	−	−
Gorkoye''	57.9	2.1	−	8.5	1	2.5	−	22.4	5.6	−	−	−
Maloye Shchuchye	92.5	0.4	−	7.1	−	−	−	−	−	−	−	−
Solenoye'	34.7	12	6.1	5.6	1.4	5.6	−	20.4	5	−	−	9.2
Shchuchye	87	0.5	−	12.5	−	−	−	−	−	−	−	−
Krugloye	78.6	2.2	2.2	5.2	1.9	−	−	5	3	−	−	1.9
Vtoroye Zasechnoye	69.6	−	−	1.5	−	5.3	−	5.4	18.2	−	−	−
Pervoye Zasechnoye	81.9	0.1	−	2.8	2.3	2.7	−	7	2.8	−	−	0.4
Solenoye''	78.1	−	1	2	2.4	1.7	−	6.4	4	−	−	4.4
Dolgoye	82.5	0.9	−	6.2	0.8	0.8	3	2.8	2.1	−	−	0.9
Belomoynoye	71.7	5.3	−	0.7	3.9	1.5	2.5	9.1	5.3	−	−	−
Medvezh'ye	75.5	2.5	1	9.7	3.7	−	3.6	−	−	4	−	−
Krotovo	72.9	−	−	25	0.7	1.4	−	−	−	−	−	−

Table A4. Cont.

Lake	Quartz	Calcite	Mg-Calcite	Feldspar	Gypsum	Aragonite	Dolomite	Illite	Hydromagnesite	Siderite	Goethite	Halite
Bol'shoye Gorkoye	59.1	10.0	1.8	17.1	4.6	7.4	–	–	–	–	–	–
Makushino	65.3	9.7	1.3	22.1	–	1.3	–	–	–	–	–	0.3
Solenoye""	69.8	6.6	0.2	20.8	–	–	–	–	–	–	–	2.6
Pritykal	78.9	1.3	0.5	18.5	–	–	–	–	–	–	–	0.8
Shashmura	53.8	24.2	–	16.2	2.2	1.3	–	–	–	–	–	2.3
Terenkol'	75.8	0.6	–	22.4	–	0.9	–	–	–	–	–	0.3
Kureynoye	57.5	14.5	2.4	17.1	5	–	0.6	–	2.9	–	–	–
Ilyeneey	94.3	1	–	3	–	–	1.7	–	–	–	–	–
Splavnoye	73.1	5	–	19.3	2.6	–	–	–	–	–	–	–
Gankino	74.9	–	–	25.1	–	–	–	–	–	–	–	–
Vasilki	53.5	0.8	7.8	6.1	–	–	–	31.8	–	–	–	–
Yakunino	29.4	10.5	12.4	5.8	5.4	4.5	–	32	–	–	–	–
Fomintsevo	53.7	–	–	15.3	23.2	–	–	–	–	–	7.8	–
Bezemyannoye	73	–	–	16	–	–	–	–	–	–	11	–
Maloye Solovoye	69	–	–	18	–	–	3	–	–	–	10	–
Mokhovoye	82	1.6	–	8	–	–	–	–	–	–	8.4	–
Maloye Kharlamovo	26.5	16.5	25	6.6	–	4.7	1	19.7	–	–	–	–
Gagar'ye	16.2	26.1	37.3	5.1	7.6	5.8	–	–	–	–	1.9	–

Note: Feldspars in total (albite, anorthite, anorthoclase).

Table A5. Results of Kruskal–Wallis one-way ANOVA by ranks and the median test for five groups of the semiarid lakes of the southwest of Western Siberia (N = 43).

Parameter	Kruskal–Wallis Test		Median Test		
	H	p	χ^2	df	p
pH	3.75	0.441	2.33	4	0.675
TDS	17.0	0.002 *	14.9	4	0.005 *
Mg ²⁺	16.9	0.002 *	16.4	4	0.003 *
Ca ²⁺	19.5	0.0006 *	14.7	4	0.005 *
Na ⁺	17.1	0.002 *	16.9	4	0.002 *
K ⁺	20.4	0.0004 *	18.8	4	0.0008 *
Cl ⁻	18.4	0.001 *	14.9	4	0.005 *
SO ₄ ²⁻	22.4	0.0002 *	16.4	4	0.003 *
DOC	14.3	0.007 *	16.4	4	0.003 *
DIC	21.1	0.0003 *	9.61	4	0.05 *

* Significant at $p < 0.05$.**Table A6.** Spearman correlation coefficients between morphological parameters of lakes and physico-chemical properties of waters (N = 43).

	Area	Watershed	Average Depth	pH	TDS	Mg ²⁺	Ca ²⁺	Na ⁺	K ⁺	Cl ⁻	SO ₄ ²⁻	DOC	DIC
Area	1												
Watershed	0.96 *	1											
Average Depth	-0.08	-0.05	1										
pH	-0.06	0.09	0.11	1									
TDS	0.49 *	-0.07	-0.26	-0.14	1								
Mg ²⁺	0.52 *	0.47 *	-0.25	-0.29	0.93 *	1							
Ca ²⁺	0.41 *	0.5 *	-0.22	-0.53 *	0.57 *	0.76 *	1						
Na ⁺	0.51 *	0.37 *	-0.26	-0.19	0.97 *	0.96 *	0.61 *	1					
K ⁺	0.46 *	0.5 *	-0.14	0.05	0.82 *	0.8 *	0.44 *	0.84 *	1				
Cl ⁻	0.52 *	0.48 *	-0.3	-0.22	0.97 *	0.95 *	0.62 *	0.98 *	0.82 *	1			
SO ₄ ²⁻	0.49 *	0.5 *	-0.33 *	-0.18	0.93 *	0.93 *	0.61 *	0.94 *	0.77 *	0.93 *	1		
DOC	0.36 *	0.48 *	-0.11	-0.04	0.9 *	0.81 *	0.4 *	0.89 *	0.86 *	0.86 *	0.79 *	1	
DIC	0.26	0.4 *	-0.01	0.07	0.65 *	0.57 *	0.15	0.67 *	0.73 *	0.64 *	0.62 *	0.75 *	1

* Significant at $p < 0.05$.

References

- Kühling, I.; Broll, G.; Trautz, D. Spatio-Temporal Analysis of Agricultural Land-use Intensity Across the Western Siberian Grain Belt. *Sci. Total Environ.* **2016**, *544*, 271–280. [\[CrossRef\]](#)
- Tkachev, B.P. *Inland Regions of the South of Western Siberia*; Tomsk State University Publ.: Tomsk, Russia, 2001. (In Russian)
- Beletskaya, N.P. Genetic Classification of Lake Basins at the West Siberian Plain. *Geomorfologiya* **1987**, *1*, 50–58. (In Russian)
- Savchenko, N.V. *Lakes of the Southern Plains of Western Siberia*; Siberian University of Consumer Cooperation: Novosibirsk, Russia, 1997. (In Russian)
- Chupina, D.A.; Zolnikov, I.D. Geoinformation Mapping of Relief Forms and Types Based on Morphometric Analysis. *Geod. I Kartogr.* **2016**, *6*, 35–43, (In Russian, English abstract).
- Bejrom, S.; Vasil'ev, I.; Gadzhiev, I. *Natural Resources of the Novosibirsk Region*; Nauka: Novosibirsk, Russia, 1986. (In Russian)
- Ovdina, E.; Strakhovenko, V.; Solotchina, E. Authigenic Carbonates in the Water—Biota—Bottom Sediments' System of Small Lakes (South of Western Siberia). *Minerals* **2020**, *10*, 552. [\[CrossRef\]](#)
- Gerasimova, E.A.; Balkin, A.S.; Filonchikova, E.S.; Mindolina, Y.V.; Zagumyonnyi, D.G.; Tikhonenkov, D.V. Taxonomic Structure of Planktonic Protist Communities in Saline and Hypersaline Continental Waters Revealed by Metabarcoding. *Water* **2023**, *15*, 2008. [\[CrossRef\]](#)
- Tranvik, L.J.; Downing, J.A.; Cotner, J.B.; Loiselle, S.A.; Striegl, R.G.; Ballatore, T.J.; Dillon, P.; Finlay, K.; Fortino, K.; Knoll, L.B.; et al. Lakes and Reservoirs as Regulators of Carbon Cycling and Climate. *Limnol. Oceanogr.* **2009**, *54*, 2298–2314. [\[CrossRef\]](#)
- Downing, J.A. Emerging Global Role of Small Lakes and Ponds: Little Things Mean a Lot. *Limnetica* **2010**, *29*, 9–24. [\[CrossRef\]](#)
- Holgerson, M.; Raymond, P. Large Contribution to Inland Water CO₂ and CH₄ Emissions from Very Small Ponds. *Nat. Geosci.* **2016**, *9*, 222–226. [\[CrossRef\]](#)
- Myrbo, A. Carbon Cycle in Lakes. In *Encyclopedia of Lakes and Reservoirs. Encyclopedia of Earth Sciences Series*; Bengtsson, L., Herschy, R.W., Fairbridge, R.W., Eds.; Springer: Dordrecht, The Netherlands, 2012; pp. 121–125. [\[CrossRef\]](#)
- Bouton, A.; Vennin, E.; Amiotte-Suchet, P.; Thomazo, C.; Sizun, J.-P.; Virgone, A.; Gaucher, E.C.; Visscher, P.T. Prediction of the Calcium Carbonate Budget in a Sedimentary Basin: A “Source-to-sink” Approach Applied to Great Salt Lake, Utah, USA. *Basin Res.* **2020**, *32*, 1005–1034. [\[CrossRef\]](#)

14. Lebedeva (Verba), M.P.; Lopukhina, O.V.; Kalinina, N.V. Specificity of the Chemical and Mineralogical Composition of Salts in Solonchak Playas and Lakes of the Kulunda Steppe. *Eurasian Soil Sci.* **2008**, *41*, 416–428. [CrossRef]
15. Mees, F.; Castañeda, C.; Van Ranst, E. Sedimentary and Diagenetic Features in Saline Lake Deposits of the Monegros Region, Northern Spain. *Catena* **2011**, *85*, 245–252. [CrossRef]
16. Last, F.M.; Last, W.M. Lacustrine Carbonates of the Northern Great Plains of Canada. *Sediment. Geol.* **2012**, *277–278*, 1–31. [CrossRef]
17. Wang, Y.; Liu, X.; Mischke, S.; Herzsuh, U. Environmental Constraints on Lake Sediment Mineral Compositions from the Tibetan Plateau and Implications for Paleoenvironment Reconstruction. *J. Paleolimnol.* **2012**, *47*, 71–85. [CrossRef]
18. Strakhovenko, V.D.; Solotchina, E.P.; Vosel', Y.S.; Solotchin, P.A. Geochemical Factors for Endogenic Mineral Formation in the Bottom Sediments of the Tazheran Lakes (Baikal Area). *Russ. Geol. Geophys.* **2015**, *56*, 1437–1450. [CrossRef]
19. Strakhovenko, V.D.; Taran, O.P.; Ermolaeva, N.I. Geochemical Characteristics of the Sapropel Sediments of Small Lakes in the Ob'-Irtys' Interfluvium. *Russ. Geol. Geophys.* **2014**, *55*, 1160–1169. [CrossRef]
20. Balci, N.; Demirel, C.; Ön, S.A.; Gültekin, A.H.; Kurt, M.A. Evaluating Abiotic and Microbial Factors on Carbonate Precipitation in Lake Acigöl, a Hypersaline Lake in Southwestern Turkey. *Quat. Int.* **2018**, *486*, 116–128. [CrossRef]
21. Cabestrero, Ó.; Sanz-Montero, M.E. Brine Evolution in Two Inland Evaporative Environments: Influence of Microbial Mats in Mineral Precipitation. *J. Paleolimnol.* **2018**, *59*, 139–157. [CrossRef]
22. De Deckker, P. Groundwater Interactions Control Dolomite and Magnesite Precipitation in Saline Playas in the Western District Volcanic Plains of Victoria, Australia. *Sediment. Geol.* **2019**, *380*, 105–126. [CrossRef]
23. Kolpakova, M.N.; Gaskova, O.L.; Naymushina, O.S.; Karpov, A.V.; Vladimirov, A.G.; Krivonogov, S.K. Saline lakes of Northern Kazakhstan: Geochemical correlations of elements and controls on their accumulation in water and bottom sediments. *Appl. Geochem.* **2019**, *107*, 8–18. [CrossRef]
24. Li, J.; Zhu, L.; Li, M.; Wang, J.; Ma, Q. Origin of Modern Dolomite in Surface Lake Sediments on the Central and Western Tibetan Plateau. *Quat. Int.* **2020**, *544*, 65–75. [CrossRef]
25. Saccò, M.; White, N.E.; Campbell, M.; Allard, S.; Humphreys, W.F.; Pringle, P.; Sepanta, F.; Laini, A.; Allentoft, M.E. Metabarcoding under Brine: Microbial Ecology of Five Hypersaline Lakes at Rottneest Island (WA, Australia). *Water* **2021**, *13*, 1899. [CrossRef]
26. Shlyapnikov, D.S.; Demchuk, N.G.; Okunev, P.V. *Mineral Components of Bottom Sediments of the Lakes of the Urals*; Ural State University: Sverdlovsk, Russia, 1990. (In Russian)
27. Novoselov, A.; Konstantinov, A.; Konstantinova, E.; Dudnikova, T.; Barbashev, A.; Lobzenko, I. Micromorphological and Mineralogical Features of Saline Playa Surface Sediments from Two Large Trans-Uralian lakes. *Eurasian J. Soil Sci.* **2022**, *11*, 93–101. [CrossRef]
28. Novoselov, A.A.; Konstantinov, A.; Lim, A.G.; Goetschl, K.; Loiko, S.V.; Mavromatis, V.M.; Pokrovsky, O.S. Mg-rich authigenic carbonates in lakes of south western Siberia: First assessment and possible mechanisms of formation. *Minerals* **2019**, *9*, 763. [CrossRef]
29. Pogoda i Klimat [Weather and Climate]. Available online: <http://www.pogodaiklimat.ru/climate.php?id=28367> (accessed on 24 September 2023).
30. Kozin, V.V.; Garmash, A.A. Landscape Structure of the Ishim Plain Central Part. *Tyumen State Univ. Herald. Nat. Resour. Use Ecol.* **2011**, *4*, 114–120, (In Russian, English summary).
31. Konstantinova, E.Y. Trace metals in soils of the main geomorphological units in the southwestern part of Western Siberia. *IOP C. Ser. Earth. Env.* **2016**, *43*, 012002. [CrossRef]
32. Puzhakov, B.A.; Saveliev, V.P.; Kuznetsov, N.S.; Shokh, V.D.; Schulkin, E.P.; Schulkina, N.E.; Zhdanov, A.V.; Dolgova, O.Y.; Tarelkina, E.A.; Orlov, M.V. Explanatory note. In *State Geological Map of the Russian Federation*; Scale 1: 1,000,000 (3rd Generation); Series Ural. Sheet N41—Chelyabinsk; Zotova, E.A., Ed.; Cartographic Factory VSEGEI: St. Petersburg, Russia, 2013. (In Russian)
33. Pokrovsky, O.S.; Shirokova, L.S.; Kirpotin, S.N.; Audry, S.; Viers, J.; Dupré, B. Effect of Permafrost Thawing on Organic Carbon and Trace Element Colloidal Speciation in the Thermokarst Lakes of Western Siberia. *Biogeosciences* **2011**, *8*, 565–583. [CrossRef]
34. Vorobyova, L.A. *Theory and Practice of Chemical Analysis of Soils*; GEOS: Moscow, Russia, 2006. (In Russian)
35. Soil Science Division Staff. *Soil survey manual. United States Department of Agriculture Handbook No. 18: U.S. Department of Agriculture*; Natural Resources Conservation Service: Washington, DC, USA, 2017.
36. Visual MINTEQ ver. 3.1. Available online: <https://vminteq.lwr.kth.se> (accessed on 25 August 2023).
37. Lawrence, G.; Siemion, J.; Antidormi, M.; Bonville, D.; McHale, M. Have Sustained Acidic Deposition Decreases Led to Increased Calcium Availability in Recovering Watersheds of the Adirondack Region of New York, USA? *Soil Syst.* **2021**, *5*, 6. [CrossRef]
38. El Ouahabi, M.; Hubert-Ferrari, A.; Fagel, N. Lacustrine Clay Mineral Assemblages as a Proxy for Land-use and Climate Changes over the Last 4 kyr: The Amik Lake Case Study, Southern Turkey. *Quatern. Int.* **2017**, *438B*, 15–29. [CrossRef]
39. Fortin, D.; Leppard, G.G.; Tessier, A. Characteristics of Lacustrine Diagenetic Iron Oxyhydroxides. *Geochim. Et Cosmochim. Acta* **1993**, *57*, 4391–4404. [CrossRef]
40. Crowe, S.A.; Roberts, J.A.; Weisener, C.G.; Fowle, D.A. Alteration of iron-rich lacustrine sediments by dissimilatory iron-reducing bacteria. *Geobiology* **2007**, *5*, 63–73. [CrossRef]
41. Novoselov, A.; Konstantinov, A.; Leonova, L.; Soktoev, B.; Morgalev, S. Carbonate Neof ormations on Modern Buildings and Engineering Structures in Tyumen City, Russia: Structural Features and Development Factors. *Geosciences* **2019**, *9*, 128. [CrossRef]

42. Areias, C.; Fernandes Barbosa, C.; Soares Cruz, A.P.; McKenzie, J.A.; Ariztegui, D.; Eglinton, T.; Haghipour, N.; Vasconcelos, C.; Sánchez-Román, M. Organic Matter Diagenesis and Precipitation of Mg-Rich Carbonate and Dolomite in Modern Hypersaline Lagoons Linked to Climate Changes. *Geochim. Cosmochim. Acta* **2022**, *337*, 14–32. [[CrossRef](#)]
43. Alibrahim, A.S.; Sodhi, R.N.S.; Duane, M.J.; Dittrich, M. Imaging of Ancient Microbial Biomarkers within Miocene Dolomite (Kuwait) Using Time-of-Flight Secondary Ion Mass Spectrometry. *Minerals* **2023**, *13*, 968. [[CrossRef](#)]
44. Power, I.M.; Wilson, S.A.; Harrison, A.L.; Dipple, G.M.; McCutcheon, J.; Southam, G.; Kenward, P.A. A Depositional Model for Hydromagnesite–Magnesite Playas near Atlin, British Columbia, Canada. *Sedimentology* **2014**, *61*, 1701–1733. [[CrossRef](#)]
45. Lin, Y.; Zheng, M.; Ye, C. Hydromagnesite Precipitation in the Alkaline Lake Dujiali, Central Qinghai-Tibetan Plateau: Constraints on Hydromagnesite Precipitation from Hydrochemistry and Stable Isotopes. *Appl. Geochem.* **2017**, *78*, 139–148. [[CrossRef](#)]
46. Scheller, E.L.; Swindle, C.; Grotzinger, J.; Barnhart, H.; Bhattacharjee, S.; Ehlmann, B.L.; Farley, K.; Fischer, W.W.; Greenberger, R.; Ingalls, M.; et al. Formation of Magnesium Carbonates on Earth and Implications for Mars. *J. Geophys. Res. Planet.* **2021**, *126*, e2021JE006828. [[CrossRef](#)]
47. Zeyen, N.; Benzerara, K.; Beyssac, O.; Daval, D.; Muller, E.; Thomazo, C.; Tavera, R.; López-García, P.; Moreira, D.; Duprat, E. Integrative Analysis of the Mineralogical and Chemical Composition of Modern Microbialites from Ten Mexican Lakes: What Do We Learn about Their Formation? *Geochim. Cosmochim. Acta* **2021**, *305*, 148–184. [[CrossRef](#)]
48. Konstantinova, E.Y. Microelements in Soils of Forest-Steppe Sequent Series in Central Part of Tobol-Ishim Interfluve. *Bull. Tomsk. Polytech. Univ. Geo Assets Eng.* **2016**, *327*, 57–66, (In Russian, English summary).
49. Zhou, S.L.; Zhang, W.C.; Wang, F. Spatial-Temporal Variations and Their Dynamics of the Saline Lakes in the Qaidam Basin Over the Past 40 Years. *IOP Conf. Ser. Earth Environ.* **2016**, *46*, 012043. [[CrossRef](#)]
50. Lengyel, E.; Pálmai, T.; Padisák, J.; Stenger-Kovács, C. Annual Hydrological Cycle of Environmental Variables in Astatic Soda Pans (Hungary). *J. Hydrol.* **2019**, *575*, 1188–1199. [[CrossRef](#)]
51. Yagmur, N.; Bilgilioglu, B.B.; Dervisoglu, A.; Musaoglu, N.; Tanik, A. Long and Short-Term Assessment of Surface Area Changes in Saline and Freshwater Lakes via Remote Sensing. *Water Environ. J.* **2020**, *35*, 107–122. [[CrossRef](#)]
52. Aydin-Kandemir, F.; Erlat, E. Assessment of the Relationship of the Salt-Covered Area and the Groundwater Storage/Drought Indicators in the Disappearing Lake Tuz in Turkey (1985–2021). *Environ. Monit. Assess.* **2023**, *195*, 333. [[CrossRef](#)] [[PubMed](#)]
53. Sui, Q.; Duan, L.; Zhang, Y.; Zhang, X.; Liu, Q.; Zhang, H. Seasonal Water Quality Changes and the Eutrophication of Lake Yilong in Southwest China. *Water* **2022**, *14*, 3385. [[CrossRef](#)]
54. Ryabogina, N.E.; Afonin, A.S.; Ivanov, S.N.; Nicolaenko, S.A.; Li, H.C.; Kalinin, P.I.; Udaltsov, S.N. Holocene Paleoenvironmental Chances Reflected in Peat and Lake Sediments Records of Western Siberia: Geochemical and Plant Macrofossil Proxies. *Quat. Int.* **2019**, *528*, 73–87. [[CrossRef](#)]
55. Ryabogina, N.E.; Yuzhanina, E.D.; Afonin, A.S.; Yakimov, A.S.; Novikov, I.K. Paleoenvironmental Studies of Lakeside Watershed Settlements of the Tobol-Ishim Interfluve (Zolotoe 1 Settlement, Kurgan Oblast). *Vestn. Arheol. Antropol. I Etnogr.* **2022**, *4*, 43–55, (In Russian, English summary). [[CrossRef](#)]
56. Krivonogov, S.K.; Zhdanova, A.N.; Solotchin, P.A.; Kazansky, A.Y.; Chegis, V.V.; Liu, Z.; Song, M.; Zhilich, S.V.; Rudaya, N.A.; Cao, X.; et al. The Holocene Environmental Changes Revealed from the Sediments of the Yarkov Sub-basin of Lake Chany, South-Western Siberia. *Geosci. Front.* **2023**, *14*, 101518. [[CrossRef](#)]
57. Manasypov, R.M.; Pokrovsky, O.S.; Kirpotin, S.N.; Shirokova, L.S. Thermokarst Lake Waters Across the Permafrost Zones of Western Siberia. *Cryosphere* **2014**, *8*, 1177–1193. [[CrossRef](#)]
58. Song, K.; Wen, Z.; Xu, Y.; Yang, H.; Lyu, L.; Zhao, Y.; Fang, C.; Shang, Y.; Du, J. Dissolved Carbon in a Large Variety of Lakes Across Five Limnetic Regions in China. *J. Hydrol.* **2018**, *563*, 143–154. [[CrossRef](#)]
59. Song, K.; Wen, Z.; Shang, Y.; Yang, H.; Lyu, L.; Liu, G.; Fang, C.; Du, J.; Zhao, Y. Quantification of Dissolved Organic Carbon (DOC) Storage in Lakes and Reservoirs of Mainland China. *J. Environ. Manage.* **2018**, *217*, 391–402. [[CrossRef](#)]
60. Curtis, P.J.; Adams, H.E. Dissolved Organic Matter Quantity and Quality from Freshwater and Saltwater Lakes in East-Central Alberta. *Biogeochemistry* **1995**, *30*, 59–76. [[CrossRef](#)]
61. Curtis, P.J.; Prepas, E.E. Trends of Dissolved Organic Carbon (DOC) Concentrations from Freshwater to Saltwater. *Verh. Internat. Verein. Limnol.* **1993**, *25*, 298–301. [[CrossRef](#)]
62. Al Disi, Z.A.; Bontognali, T.R.R.; Jaoua, S.; Attia, E.; Al-Kuwari, H.A.S.; Zouari, N. Influence of Temperature, Salinity and Mg^{2+} : Ca^{2+} Ratio on Microbially-Mediated Formation of Mg-Rich Carbonates by *Virgibacillus* Strains Isolated from a Sabkha Environment. *Sci. Rep.* **2019**, *9*, 19633. [[CrossRef](#)] [[PubMed](#)]
63. Pan, Y.; Li, Y.; Ma, Q.; He, H.; Wang, S.; Sun, Z.; Cai, W.-J.; Dong, B.; Di, Y.; Fu, W.; et al. The Role of Mg^{2+} in Inhibiting $CaCO_3$ Precipitation from Seawater. *Mar. Chem.* **2021**, *237*, 104036. [[CrossRef](#)]
64. Han, Z.; Qi, P.; Zhao, Y.; Guo, N.; Yan, H.; Tucker, M.E.; Li, D.; Wang, J.; Zhao, H. High Mg/Ca Molar Ratios Promote Protodolomite Precipitation Induced by the Extreme Halophilic Bacterium *Vibrio harveyi* QPL2. *Front. Microbiol.* **2022**, *13*, 821968. [[CrossRef](#)] [[PubMed](#)]
65. Zeyen, N.; Daval, D.; Lopez-Garcia, P.; Moreira, D.; Gaillardet, J.; Benzerara, K. Geochemical Conditions Allowing the Formation of Modern Lacustrine Microbialites. *Procedia Earth Planet. Sci.* **2017**, *17*, 380–383. [[CrossRef](#)]
66. Runnegar, B. The Evolution of Mineral Skeletons. In *Origin, Evolution, and Modern Aspects of Biomineralization in Plants and Animals*; Crick, R.E., Ed.; Springer: Boston, MA, USA, 1989; pp. 75–94. [[CrossRef](#)]

67. Bischoff, K.; Sirantoine, E.; Wilson, M.E.; George, A.D.; Mendes Monteiro, J.; Saunders, M. Spherulitic Microbialites from Modern Hypersaline Lakes, Rottneest Island, Western Australia. *Geobiology* **2020**, *18*, 725–741. [[CrossRef](#)]
68. Braithwaite, C.J.R.; Zedef, V. Hydromagnesite Stromatolites and Sediments in an Alkaline Lake, Salda Golu, Turkey. *J. Sediment. Res.* **1996**, *66*, 991–1002. [[CrossRef](#)]
69. Renaut, R.W. Morphology, Distribution, and Preservation Potential of Microbial Mats in the Hydromagnesite-Magnesite Playas of the Cariboo Plateau, British-Columbia, Canada. *Hydrobiologia* **1993**, *267*, 75–98. [[CrossRef](#)]
70. Coshell, L.; Rosen, M.R.; McNamara, K.J. Hydromagnesite Replacement of Biomineralized Aragonite in a New Location of Holocene Stromatolites, Lake Walyungup, Western Australia. *Sedimentology* **1998**, *45*, 1005–1018. [[CrossRef](#)]
71. Sanz-Montero, M.E.; Cabestrero, Ó.; Rodríguez-Aranda, J. Hydromagnesite Precipitation in Microbial Mats from a Highly Alkaline Lake, Central Spain. *Miner. Mag* **2013**, *77*, 2133.
72. Sanz-Montero, M.E.; Cabestrero, Ó.; Sánchez-Román, M. Microbial Mg-rich Carbonates in an Extreme Alkaline Lake (Las Eras, Central Spain). *Front. Microbiol.* **2019**, *10*, 148. [[CrossRef](#)] [[PubMed](#)]
73. Shirokova, L.S.; Mavromatis, V.; Bundeleva, I.A.; Pokrovsky, O.S.; Bénézech, P.; Gérard, E.; Pearce, C.R.; Oelkers, E.H. Using Mg isotopes to trace cyanobacterially mediated magnesium carbonate precipitation in alkaline lakes. *Aquat. Geochem.* **2013**, *19*, 1–24. [[CrossRef](#)]
74. Balci, N.; Gunes, Y.; Kaiser, J.; On, S.A.; Eris, K.; Garczynski, B.; Horgan, B.H. Biotic and Abiotic Imprints on Mg-Rich Stromatolites: Lessons from Lake Salda, SW Turkey. *Geomicrobiol. J.* **2020**, *37*, 401–425. [[CrossRef](#)]
75. Kaya, M.; Yildirim, B.A.; Kumral, M.; Sasmaz, A. Trace and Rare Earth Element (REE) Geochemistry of Recently Formed Stromatolites at Lake Salda, SW Turkey. *Water* **2023**, *15*, 733. [[CrossRef](#)]
76. Maltsev, A.E.; Leonova, G.A.; Bobrov, V.A.; Krivonogov, S.K.; Miroshnichenko, L.V.; Vossel, Y.S.; Melgunov, M.S. Geochemistry of Carbonates in Small Lakes of Southern West Siberia Exemplified from the Holocene Sediments of Lake Itkul'. *Rus. Geol. Geoph.* **2020**, *61*, 303–321. [[CrossRef](#)]
77. Solotchin, P.A.; Solotchina, E.P.; Maltsev, A.E.; Leonova, G.A.; Krivonogov, S.K.; Zhdanova, A.N.; Danilenko, I.V. Carbonate Sedimentation in High-Mineralized Lake Bolshoi Bagan (South of West Siberia): Dependence on Holocene Climate Changes. *Russ. Geol. Geophys.* **2023**, *64*, 1098–1107. [[CrossRef](#)]
78. Chen, X.; Meng, X.; Song, Y.; Zhang, B.; Wan, Z.; Zhou, B.; Zhang, E. Spatial Patterns of Organic and Inorganic Carbon in Lake Qinghai Surficial Sediments and Carbon Burial Estimation. *Front. Earth Sci.* **2021**, *9*, 714936. [[CrossRef](#)]
79. Serikova, S.; Pokrovsky, O.S.; Laudon, H.; Krickov, I.V.; Lim, A.G.; Manasypov, R.M.; Karlsson, J. High carbon emissions from thermokarst lakes of Western Siberia. *Nat. Commun.* **2019**, *10*, Art No 1552. [[CrossRef](#)]
80. Manasypov, R.M.; Lim, A.G.; Aliev, V.; Shevchenko, V.P.; Shirokova, L.S.; Karlsson, J.; Pokrovsky, O.S. Carbon and nitrogen storage in thermokarst lake sediments of WSL peatlands: Impact of climate, permafrost and lake size. *Biogeochemistry* **2022**, *159*, 69–86. [[CrossRef](#)]

Disclaimer/Publisher's Note: The statements, opinions and data contained in all publications are solely those of the individual author(s) and contributor(s) and not of MDPI and/or the editor(s). MDPI and/or the editor(s) disclaim responsibility for any injury to people or property resulting from any ideas, methods, instructions or products referred to in the content.